Journal of
Medicinal Chemistry

Article

Synthesis, pharmacological characterization, and structure-activity relationships of non-canonical selective agonists for #7 nAChRs

Gisela Andrea Camacho-Hernandez, Clare Stokes, Brendan M. Duggan, Katarzyna Kaczanowska, Stefania Brandao-Araiza, Lisa Doan, Roger L. Papke, and Palmer Taylor

J. Med. Chem., **Just Accepted Manuscript** • DOI: 10.1021/acs.jmedchem.9b01467 • Publication Date (Web): 01 Nov 2019

Synthesis, pharmacological characterization, and structure-activity relationships of non-canonical selective agonists for α7 nAChRs

Gisela Andrea Camacho-Hernandez[†], Clare Stokes[‡], Brendan M. Duggan[†], Katarzyna Kaczanowska[†], Stefania Brandao-Araiza[†], Lisa Doan[†], Roger L. Papke[‡], and Palmer Taylor[†*].

†Department of Pharmacology, Skaggs School of Pharmacy & Pharmaceutical Sciences, University of California-San Diego, La Jolla, CA 92093-0751. ‡Department of Pharmacology & Therapeutics, University of Florida, PO Box 100267, Gaines ville FL, 32610-0267.

KEYWORDS Selective agonists, substituted pyrimidines, nicotinic acetylcholine receptors, ligand-gated ion channels, NMR pKa analysis

ABSTRACT: A lack of selectivity of classical agonists for the nicotinic acetylcholine receptors (nAChR) has prompted us to identify and develop a distinct scaffold of α7 nAChR-selective ligands. Non-canonical 2,4,6-substituted pyrimidine analogues were framed around compound 40 for a structure-activity relationship study. The new lead compounds activate selectively the α7 nAChRs with EC50's between 30-140 nM in a PNU-120596-dependent, cell-based calcium influx assay. After characterizing the expanded lead landscape, we ranked the compounds for rapid activation using *Xenopus* oocytes expressing human α7 nAChR with a two-electrode voltage clamp. This approach enabled us to define the molecular determinants governing rapid activation, agonist potency, and desensitization of α7 nAChRs after exposure to pyrimidine analogues, thereby distinguishing this subclass of non-canonical agonists from previously defined types of agonists (agonists, partial agonists, silent agonists, and ago-PAMs). By NMR, we analyzed pKa values for ionization of lead candidates, demonstrating distinctive modes of interaction for this landscape of ligands.

INTRODUCTION

Nicotinic acetylcholine receptors (nAChRs) belong to a pentameric ligand-gated ion channel superfamily and are among the most well-studied allosteric transmembrane signaling proteins.[1-2] They are sub-classified as muscle and neuronal receptors, and the latter are widely distributed in the peripheral autonomic and the central nervous systems, as well as in some non-neuronal cell types. nAChRs are predominantly found in brain on presynaptic terminals modulating the release of other neurotransmitters.[3] The orthosteric and allosteric sites and functions of nAChRs have made them potential candidate targets for treating progressive brain disorders of aging and development such as Alzheimer's,[4-6] Parkinson's,[7-8] and schizophrenia,[9-10] as well as inflammation.[11] One of the most abundant neuronal nAChRs is the homopentameric α7 subtype. As such, it is comprised of five identical α7 subunits with five potential orthosteric binding sites, which are located at the respective subunit interfaces of the extracellular domain. The α7 nAChR has unique pharmacological recognition and electrophysiological response properties when compared to other subtypes; for example, it retains relatively low affinity for nicotine or acetylcholine in the desensitized state, is activated by choline, displays high permeability for calcium, and exhibits rapid desensitization when exposed to high concentrations of agonist.[12-13] The α7 nAChR is known to be highly expressed in the hippocampus and prefrontal cortex, where it modulates cognition, sensory processing, working memory, and attention.[14-15] Activation of this subtype of nAChR can enhance attention and cognition in animal models.[10,15] More recently the α7 nAChR has been explored as a target for inflammation via metabotropic activation in immune cells where it regulates the cholinergic anti-inflammatory pathway (CAP).[11,16-18]

Ligand binding to the orthosteric binding site of neuronal and non-neuronal nAChRs requires a cationic center and usually a hydrogen bond donor or acceptor.[19] Horenstein *et al*. reported three chemical motifs to achieve α7 nAChR selectivity: the benzylidene motif, tropane motif, and choline motif.[20] Incorporating a hydrophobic feature, such as a single methyl, as with tropane, or a large aromatic group such as the benzylidene in GTS-21,[5,9] in addition to a cationic center can convert a non-selective agonist into a more α7-selective drug. Despite these considerations, more detailed clinical studies have often resulted in leads lacking sufficient selectivity among other nAChR subtypes and a 5-hydroxytryptamine (5-HT_{3A}) ion channel receptor. Accordingly, critical side effects or limited efficacy at the doses used become manifest. GTS-21,[5,9] MEM3454 (RG3487),[15,21] Encenicline (EVP-6124),[22] and TC-5619[10,23] are examples of leads with these characteristics that have been brought to Phase 1 and 2 clinical trials (Figure 1).

In previous work,[24] we identified a small sub-group of 4,6-disubstituted-2-aminopyrimidines that interact with the acetylcholine binding protein (AChBP)[25-26] and selectively activate α7 nAChRs in a cell-based calcium influx assay.[27]

Moreover, these ligands are structurally distinct from classical nicotinic agonists, where the nitrogens residing on the pyrimidine and pyridine rings all are weakly basic. We hypothesize, based on the structures, when compared to prototypical agonists, that these ligands show limited protonation at physiological pH, thus minimizing classical cation-π interactions.[28] Furthermore, a cell-based calcium influx assay has a prolonged time-frame, so inclusion of a type II positive allosteric modulator (PAM), such as PNU-120596 was required for signal detection. An open question remains as to whether these compounds activate the α7 nAChR in the absence of PNU-120596 and, accordingly, differ from silent agonists[18,29] or ago-PAMs.[30-31] Our current measurements in the oocyte system not only indicate agonist activity without the presence of PNU-120596, but also reveal that the kinetics of activation, efficacy, and recovery from desensitization differ within this pyrimidine sub-family from the classic α7 nAChR agonists described to date.

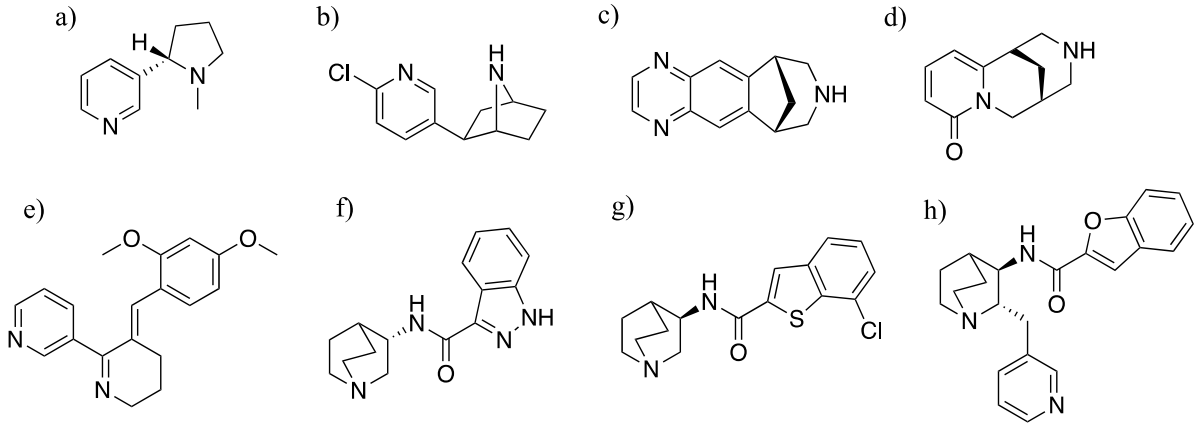

Figure 1. Examples of nAChR ligands: a) (-)-Nicotine, b) (±)-Epibatidine, c) Varenicline, d) Cytisine. Examples of nAChR ligands with selective α7 nAChR agonist activation: e) GTS-21,[5,9] f) MEM3454 (RG3487),[15,21] g) Encenicline (EVP-6124),[22] h) TC-5619.[10,23]

Scheme 1. Synthesis of compounds 56-66 (for structures see Table 1).

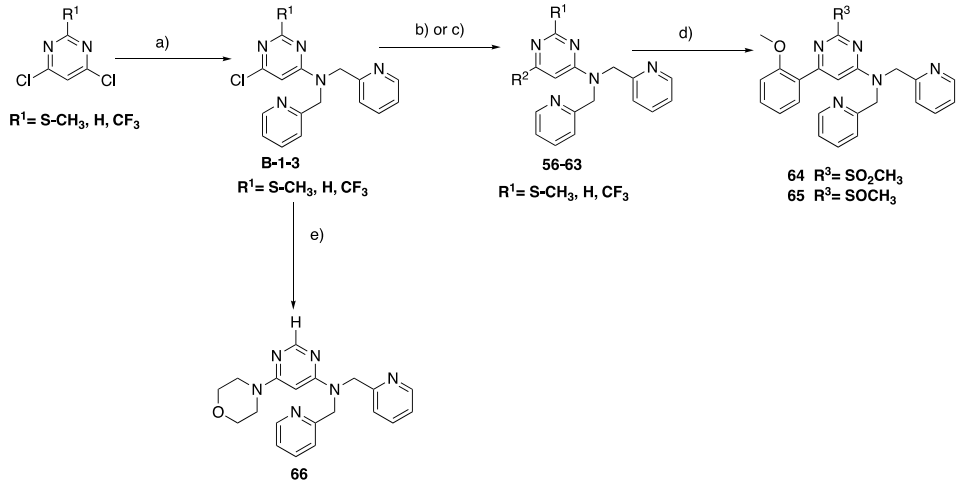

Reagents and conditions: a) di-(2-picolyl) amine, DIPEA, DMF, 80 °C; b) boronic acid, $Pd(dppf)Cl_2$, K_2CO_3, DMA, 149 °C; c) boronic acid, $Pd(PPh_3)_4$, Na_2CO_3, THF, reflux; d) 1 eq. or 2 eq. of m-CPBA in DCM, 0 °C; e) morpholine, DIPEA, 2-propanol, microwave irradiation, 160 °C.

RESULTS AND DISCUSSION

Synthetic strategies and distinguishing chemistry. Based on our crystallographic studies with AChBP,[24] in complex with the di-(2-picolyl) amine ligand series, we identified key ligand features for influencing AChBP affinity. Along with di-(2-picolyl) amine system capturing carbonyl and indole regions of Trp143 of *Ls*AChBP, major contributions were attributed to the pyrimidine ring nitrogen and the pyrimidine position 2 NH_2 substituent. With the understanding of importance of the two latter positions, we modified the 2 position by introducing relatively small functional groups with varying electronic influences. Starting with symmetric commercially available pyrimidine precursors, aromatic nucleophilic substitution was performed with 4,6-dichloro-2-(methylthio)pyrimidine, 4,6-dichloropyrimidine, or 4,6-dichloro-2-(trifluoromethyl)pyrimidine to obtain intermediate **B-1 (**91% yield**), B-2 (**64% yield), or intermediate **B-3 (**93% yield), respectively. Cross-coupling Suzuki reactions utilizing a choice of boronic acid, $Pd(dppf)Cl_2$, and as a base K_2CO_3 in *N,N*-dimethylacetamide (DMA) yielded compounds **56-59, 62-63** (Table 1). For compounds **60-61** (Table 1) different coupling conditions

were used, namely $Pd(PPh_3)_4$ as a catalyst, Na_2CO_3 as a base in THF. A total of eight compounds were synthesized via these two steps. Compounds **64-65** (Table 1) required an additional oxidation step using *m*-CPBA (Scheme 1).

Recognizing the importance of the di-(2-picolyl) amine substituent, we confirmed the need for both pyridines that maintain an axis of symmetry in this part of the structure. Following this concept, we synthesized compound **75** (Scheme 2, Table 1). An additional step was added to assemble *N*-benzyl-1-(pyridin-2-yl)methanamine by a direct reductive amination that afforded **B-4**. Purification of this amine presented a challenge, where the best option seemed to be utilizing oxalic acid to generate the protonated secondary amine. After isolation in 67% yield, the amine was reacted with 2-amino-4,6-dichloropyrimidine to give intermediate **B-5** in 36% yield. Suzuki coupling was performed utilizing $Pd(dppf)Cl_2$ and K_2CO_3 in DMA to yield 83% of a white solid compound **75** (Scheme 2). Based on the previous lead, compound **40**, we continued to expand our landscape with modifications in the position 6. Initially, we sampled mostly the *-ortho* position of the aromatic substituent in combination with different variants of the *-para* substituents. Our intent was to increase hydrophobicity in this part of the structure, as, according to the earlier studies, this substitution emerged as an important feature to achieve selectivity with respect to other nicotinic receptors.[20] Synthesis of **B-21** intermediate has been previously described.[24] Coupling condition (b) was utilized to obtain compounds **67-69** (Table 1) and **71-72** (Table 1) in good to excellent yields. In the case of compound **70,** no traces of the expected product were observed leading to reaction conditions modification by applying $Pd(PPh_3)_4$ as a catalyst, and Na_2CO_3 as a base in THF. Compound **70** (Table 1) was successfully obtained albeit in low, 27% yield. Similar coupling conditions were used to produce compounds **73-74** (Table 1)

Since basicity of the pyrimidine nitrogen in the series should be affected by the adjacent substituent in position 6, we introduced a non-aromatic moiety to increase the pKa in the pyrimidine (calculations performed in MarvinSketch 17.27). Consequently, in compound **66** (Table 1), we introduced a morpholine as a substituent via an aromatic substitution performed under microwave irradiation.[32]

Scheme 2. Modifications at pyrimidine position 6.

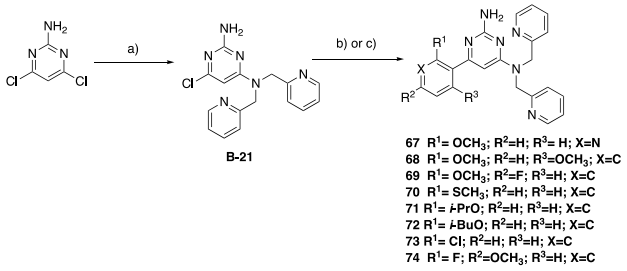

Reagents and conditions: a) di-(2-picolyl amine), DIPEA, DMF, 80 °C; b) boronic acid, $Pd(dppf)Cl_2$, K_2CO_3, DMA, 149 °C; c) boronic acid, $Pd(PPh_3)_4$, Na_2CO_3, THF, reflux.

Scheme 3. Modification at pyrimidine position 4.

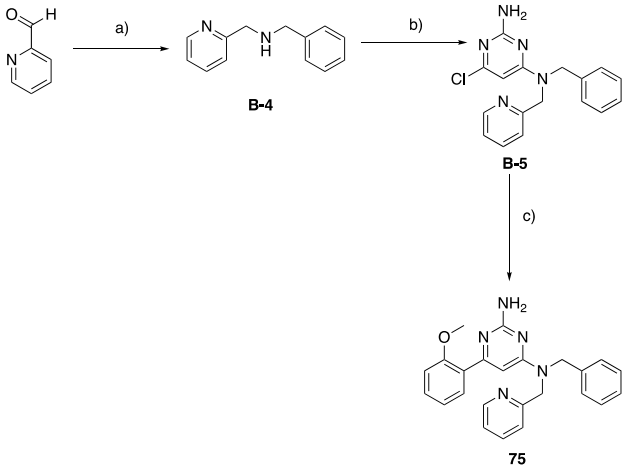

Reagents and conditions: a) benzylamine, $NaBH_4$ EtOH, 0 °C; b) 2-amino-4,6-dichloropyrimidine, DIPEA, DMF, 80 °C; c) 2-methoxyphenyl boronic acid, $Pd(dppf)Cl_2$, K_2CO_3, DMA, 149 °C.

Effects of divergent substitutions, using nAChR cell-based neurotransmitter fluorescent engineered reporters (CNiFERs) for structure-activity analysis.

As a screen of moderate throughput, and as a first analyzing step, we utilized HEK stable cell lines expressing α7 and α4β2 nAChRs and 5-HT_{3A} receptors with the TN-XXL calcium reporter biosensor.[27] The CNiFERs measure changes in fluorescence by Ca^{2+} binding as a result of Ca^{2+} influx from agonist activation. Due to the desensitizing profile of α7 nAChR, PNU-120596 was required in initial α7 nAChR screens. Saturation of genetically encoded fluorescence biosensor can occur, and this may lead to a misinterpretation of efficacy and potency; therefore, we treated this evaluation as a first step to detect well-suited candidates for electrophysiologic analysis.

Out of twenty-three present compounds, nineteen activated the human α7 nAChRs; accordingly activation was normalized to a 316 nM response of (±)-Epibatidine (Figure 2). As a preliminary structure-activity relationship (SAR) analysis and to explore how different substitutions in the 2-position affect the response, we compared compound **40**[24] (EC_{50}= 70 nM) with compounds **56** (EC_{50}= 110 nM), **58** (EC_{50}= 140 nM), and **62** (EC_{50}= 530 nM). A decrement of 2- to 8-fold in potency and a modest decrement in the efficacy were observed (Table 1, Figure 2A). In our previous study,[24] utilizing the structural surrogate *Ls*-AChBP in complex with compound **40** (PDB ID 5j5h), we observed a 2.5-3.5Å hydrogen bonding distance from the conserved Tyr 164 in the α7 nAChR to the NH_2 group. Although the same interaction might not be present in compounds **56** and **58,** compounds **62**, **64**, and **65** should form hydrogen bonds,[33-34] perhaps constrained by parameters of distance, geometry, and molecular dimensions. Compounds **57** (EC_{50}= 1.8 μM), **59** (EC_{50}= 2.1 μM), and **63** (EC_{50}= 2.5 μM), when compared to compound **44**[24] (EC_{50}= 500 nM), present a ~4-fold

decrease in potency, underlining sensitivity of this region of the complex and appropriate heterocyclic aromatic group in the position 6, and the stabilization by an additional hydrogen bond in position 2 to increase potency. When the aromatic group was replaced by the non-aromatic heterocyclic moiety in **66**, a diminished interaction was detected in all the three different cell lines, despite increased basicity of the pyrimidine ring nitrogen compared to analogs **58-61**, (MarvinSketch pKa 6.75 for **66,** 4.56 for **58**, 4.71 for **59**, 3.53 for **60** and 3.48 for **61**). This suggested that basicity of the pyrimidine ring nitrogen does not suffice for this series to maintain affinity/potency to the studied receptors. Rather, the ligand system requires additional hydrophobic interactions offered by aromatic substituents in the position 6 of the pyrimidine ring. A similar loss of agonist activity was found by symmetry disruption in the di-2-picolyl system. As demonstrated for compound **75**, activation of α7 nAChRs was abolished up to concentrations as high as 13.3 μM, confirming the need for a bidentate system, such as the di-(2-picolyl) group, to achieve activation. Interestingly, compound **75** inhibited both α4β2 nAChR and 5-HT_{3A} receptors. The di-(2-picolyl) moiety appears as a key pharmacophore feature for α7 nAChR activation but not necessarily antagonism. When the 2-NH_2 group was replaced by hydrophobic moieties in **56** and **62**, antagonism of α4β2 nAChR and 5-HT_{3A} serotonin receptors increased. Compounds **64** and **65** exhibited approximately 7-fold decreases in potency and maintained the selectivity to some degree, suggesting that large polar substituents at position 2 of the pyrimidine reduce potency (Table 1, Figure 2A).

An increase in hydrophobicity and atom size at the -*ortho* position of the phenyl substituent in position 6 of the pyrimidine ring led to an increment in antagonism of α4β2 nicotinic and 5-HT_{3A} receptors, as well as a loss in potency in α7 nAChRs (**40** vs **71** and **72**, Table 1, Figure 2B). Substitution with fluorine in compound **74** was aimed at maintaining hydrogen bond accepting properties at the -*ortho* position while modulating lipophilicity of the ligand. Ligand **74** gave increased potency compared to **41**, with an EC_{50} of 30 nM. The key replacement in compound **74** was a swap of a methoxy group for a fluorine. Fluorine can act as a bio-isostere of a methoxy group if the binding pocket can accommodate the CH_3 group.[35] A fluorine substitution often leads to improved permeability and metabolic stability, both parameters are of great importance to drug development.[35-36]

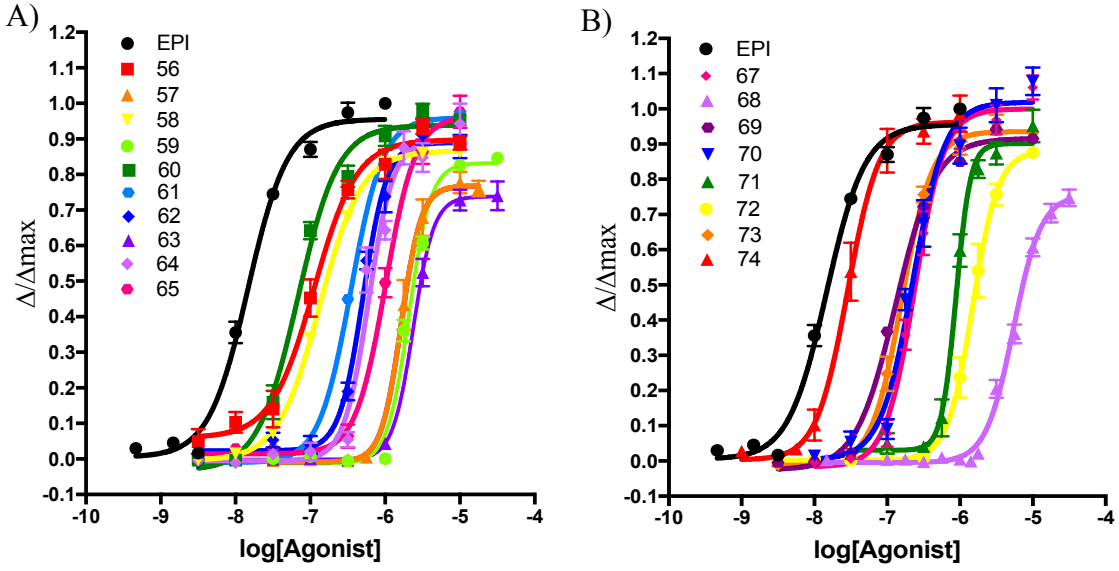

Figure 2. α7 nAChR concentration-response curves in the presence of PNU-120596 of a series of 2,4,6-trisubstituted pyrimidines performed with HEK cells containing a calcium-sensitive fluorescence reporter.

TABLE 1. Functional parameters, α7 nAChR $EC_{50,}$ and antagonist dissociation constants, K_A, for α4β2 nAChR and 5-HT_{3A} receptors.

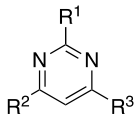

Compound	R^1	R^2	R^3	Agonist EC_{50} ± SD (μM)	Antagonist K_A ± SD (μM)	
				α7 nAChR	α4β2 nAChR	5-HT_{3A}
40*	NH_2		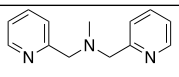	0.07 ± 0.01	6.3 ± 1.5	>10

41*	**NH_2**	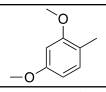	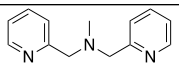	0.07 ± 0.01	2.5 ± 0.8	>10
44*	**NH_2**		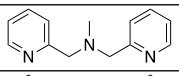	0.5 ± 0.1	>10	>10
56	**SCH_3**		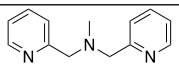	0.11 ± 0.02	1.1 ± 0.2	2.8 ± 0.6
57	**SCH_3**		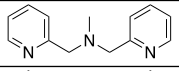	1.8 ± 0.5	3.4 ± 1.5	2.2 ± 0.8
58	**H**		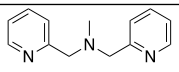	0.14 ± 0.02	7.9 ± 0.9	>10
59	**H**		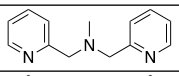	2.1 ± 0.2	>10	>10
60	**H**	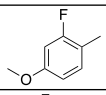	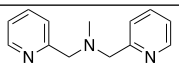	0.069 ± 0.0003	3.0 ± 1.2	5.4 ± 1.1
61	**H**		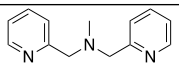	0.36 ± 0.07	5.6 ± 1.1	8.4 ± 1.1
62	**CF_3**		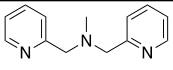	0.53 ± 0.06	1.7 ± 0.3	3.7 ± 0.8
63	**CF_3**		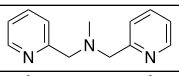	2.5 ± 0.3	0.96 ± 0.2	3.6 ± 1.3
64	**SO_2CH_3**		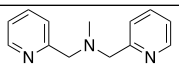	0.69 ± 0.06	7.2 ± 1.9	>10
65	**$SOCH_3$**		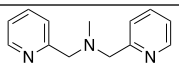	0.92 ± 0.2	>10	>10
66	**H**		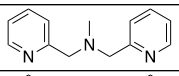	>13.3	>10	>10
67	**NH_2**		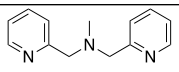	0.23 ± 0.05	>10	>10
68	**NH_2**	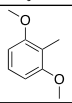	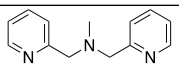	5.4 ± 1.0	7.1 ± 0.9	>10
69	**NH_2**		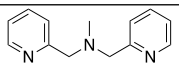	0.12 ± 0.04	4.8 ± 0.8	>10
70	**NH_2**		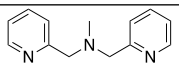	0.24 ± 0.03	4.3 ± 1.5	>10
71	**NH_2**	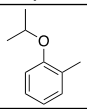	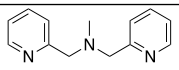	0.89 ± 0.07	1.5 ± 0.4	>10
72	**NH_2**	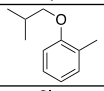	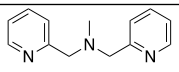	1.6 ± 0.5	1.3 ± 0.4	5.5 ± 0.5
73	**NH_2**		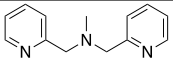	0.16 ± 0.03	3.4 ± 0.9	>10
74	**NH_2**			0.03±0.009	3.2 ± 1.3	5.3 ± 0.5
75	**NH_2**			>13.3	1.3 ± 0.6	4.1 ± 0.6

[1]Dissociation constants are based on non-competitive antagonism. α4β2 nAChR analysis was made without distinguishing subunit stoichiometry. Responses are measured from at least three independent experiments in HEK cells containing a fluorescence reporter and plated as monolayers on 96-well plate. * Previously described compounds.[24]

Electrophysiological analysis

Based on CNiFERs results, four compounds were selected for fast activation analysis: compounds **58**, **60**, and **74**, in addition to the previously described[24] compound **40**. Electrophysiological characterization was performed in *Xenopus* oocytes expressing human neuronal α7 nAChR with two-electrode voltage clamp. Initially, the four compounds were tested at 30 μM (Figure 3); the test responses were normalized to the average of two 60 μM ACh pre-control responses for each oocyte. A single-concentration analysis, when an appropriate concentration is used, can provide information of potency and efficacy based on the peak-current to net-charge ratio, and facilitates a further concentration-response analysis.[37] The four compounds activated α7 nAChR at the standard single concentration; peak current measurements were compared, and the responses were significantly larger for all compounds than for the 60 μM ACh controls (Figure 3), reflecting high potency of the four compounds.[37] After a washing period of 181 s with Ringer's solution, 60 μM ACh was applied, and minimal activation of the receptor was detected for all compounds (Figure 3), suggesting a low recovery of the receptor and potentially a stabilization of a closed channel, desensitized state. The type II PAM PNU-120596 affects the peak-current responses and the kinetics of the agonist response by binding to the transmembrane domain and destabilizing some of the desensitized states.[38] Therefore, to demonstrate whether the pyrimidine analogs induced stabilization of a PAM-sensitive closed, desensitized state (D_s), 10 μM PNU-120596 was then applied. As shown in Figure 3**,** the receptors desensitized by the four compounds responded to PNU-120596, with compounds **58**, **60**, and **74** showing marked increase over the 60 μM ACh pre-control responses. Despite the stabilization of a PAM-sensitive D_s state by these compounds, thereby resembling silent agonists, the pyrimidines differ by having significant activation when PNU-120596 is absent.

An alternative allosteric binding site in the extracellular vestibule of the α7 nAChR has been suggested to be involved with PNU-dependent reactivation of desensitized receptors[39]. This site was first identified as being one of two binding sites recognized by the ago-PAM GAT107, the other site being a site in the transmembrane domains that is shared with other PAMs such as PNU-120596 or TQS.[40] A further detailed electrophysiological analysis, outside the scope of the present study, indicates that the 2,4,6-substituted pyrimidine analogues may also depend on this allosteric activation site. Concentration-response curves of selected compounds are shown in Figure 4a, based on net-charge, rather than peak-current, analysis. Due to the rapid desensitization of α7 receptors by high agonist concentrations, peak currents often occur before completing application of drug, so that increases in peak current do not reflect increased receptor activation, but rather synchronization of channel opening events.[41] Net charge analysis avoids this artifact. These results are consistent with single-concentration analysis; compound **74** was the most potent with an EC_{50} of 0.11 ± 0.03 μM with and I_{max} = 0.84 ± 0.03 of the ACh maximum, followed by compound **40** with an EC_{50} of 0.35 ± 0.11μM and I_{max}= 0.98 ± 0.08. Compound **60** showed a partial agonist profile with an EC_{50} of 0.60 ± 0.15 μM and I_{max}= 0.53 ± 0.04.

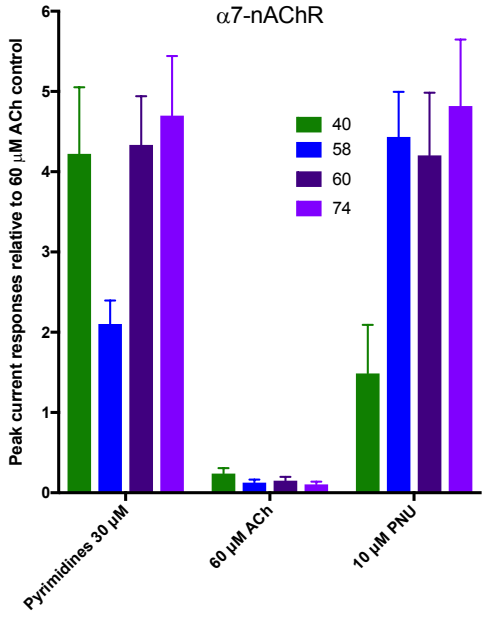

Figure 3. Peak current responses to 30 μM of selected lead compounds **40**, **58**, **60**, and **74** followed by application of 60 μM ACh and then 10 μM PNU-120596 performed in *Xenopus* oocytes expressing human α7 nAChRs. Compound applications were 12 sec duration, followed by 211-second washout periods. Experimental values are the mean responses (± SEM) of six cells, each scaled to their respective ACh pre-controls.

The least potent compound analyzed electrophysiologically was compound **58,** with an EC_{50} of 3.35 ± 0.68 μM showing a full agonistic profile with an I_{max} = 0.89 ± 0.07. All compounds followed the same potency order in single-concentration analysis and the calcium CNiFERs assay, suggesting that the NH_2 group in position 2 enhances potency. Characterization of the inhibition was made by adding a single concentration of ACh, 60 μM, post-application of compounds (Figure 4b). Inhibition followed the potency order: compound **74** with an IC_{50}= 0.47 ± 0.20, **40** IC_{50}=0.37 ± 0.15, **60** IC_{50}= 1.3 ± 0.30 and, **58** IC_{50}= 3.5 ± 1.0μM, confirming the binding of these compounds in the orthosteric site.

To increase our selectivity profile and confirm previous CNiFERs results with α4β2 nAChR, all compounds were assayed at 30 μM against four heteromeric receptors: the stoichiometry differing between the human high sensitivity (HS) and low sensitivity (LS) forms of α4β2,[42] α3β4, and the mouse muscle α1β1εδ nAChRs, all expressed in *Xenopus* oocytes utilizing the two-electrode voltage clamp system. The four compounds showed high selectivity for the α7 subtype with minimal to no activation on heteromeric nAChRs (Figure 5), confirming our previous findings. Compound **40** showed more inhibition of the four receptors when co-applied with ACh, especially in mouse muscle α1β1εδ and human α3β4 nAChR (Figure 5). Structurally, pyrimidine analogs **40** and **74**, with NH_2 in the position 2,

appeared to inhibit the α1β1εδ and α3β4 nAChRs more than their two congeners, **58** and **60**. There was no notable preference for inhibition of one of the two isoforms of α4β2 n-AChR. When recovery of the receptor was assessed by control application of ACh (30μM for α1β1εδ, 100 μM for α3β4, 100 μM for LS α4β2, and 10 μM for HS α4β2), α3β4 and the LS and HS forms of α4β2 nAChRs appeared to recover faster than the muscle receptor, which remained inhibited after the wash period (figure 5).

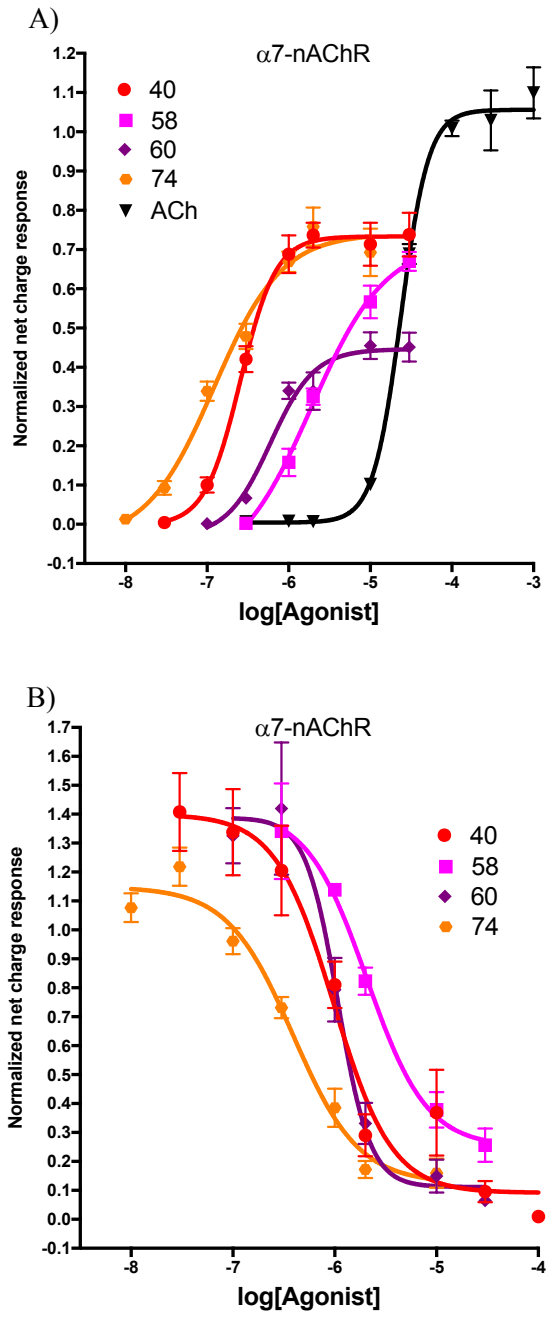

Figure 4. a) Concentration-response curves of α7 nAChR for selected compounds **40**, **58**, **60**, and **74**. The responses are normalized to 60 μM ACh; experimental values are the averaged responses (±SEM) of six cells. b) Inhibition concentration-response curves (iCRC) of α7 nAChR for selected compounds **40**, **58**, **60**, and **74,** when tested by a post application of 60 μM ACh (see Figure 3 for details).

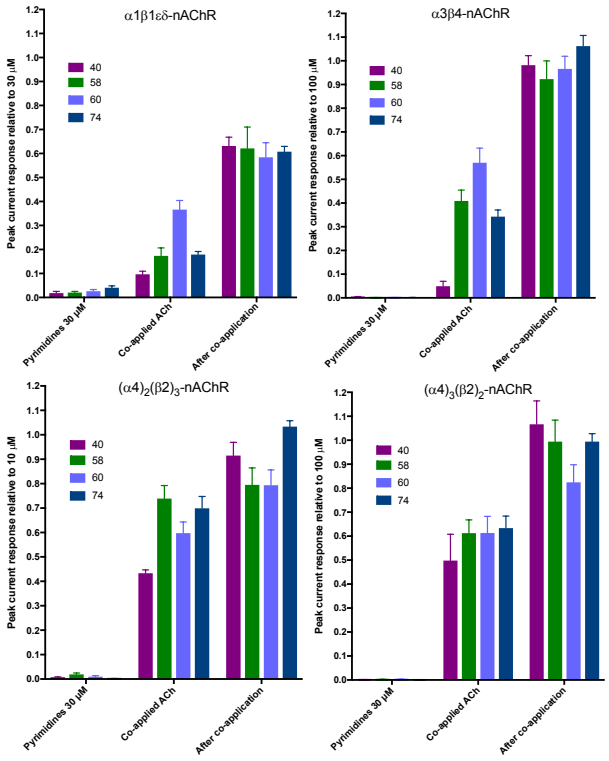

Figure 5. Electrophysiological evaluation of compounds **40**, **58**, **60**, and **74** in heteropentameric nAChRs performed in *Xenopus* oocytes. Compound applications were 6 seconds duration, followed by a 271-second washout period. The control concentrations of ACh were 30 μM for α1β1εδ, 100 μM for α3β4, 100 μM for LS α4β2, and 10 μM for HS α4β2. After experimental drug applications, follow-up control applications of ACh were made to test prior pyrimidine exposures.

pKa determinations and *in silico* phisico-chemical properties

pKa values were determined utilizing ^{1}H-NMR by measuring chemical shifts when neighboring nuclei protonate[43-44]. This technique has been reported to be a highly reliable alternative for pKa assessments when compared to UV-spectroscopy, potentiometric measurements, or *in silico* estimates.[45-46] Our samples were prepared in phosphate buffer over pH ranges of 1.85-9.56 for nicotine, 2.62-8.51 for compounds **40** and **74**, and 2.65-7.53 for compound **60.** No D_2O to suppress the H_2O signals was employed to avoid changes in the chemical shifts. Compound **40** was prepared at a final concentration of 1 mM and compounds **60** and **74** at 0.25 mM. Nicotine was used as a control; final concentration over the pH range 9.56-3.28 was 20 mM; 10 mM of nicotine was utilized from pH 3.61 to 1.85. Chemical shifts were plotted against pH forming a sigmoidal curve (supplemental information). pKa's were obtained from the inflection points as previously described;[44] pKa's and standard deviations are reported as means when 2 or more vicinal hydrogens were plotted. We did not measure values below pH 2.65 to avoid compound degradation. This

did not allow us to reach the plateau of the sigmoidal curve for compound **60** (supplemental information).

Compounds **40** and **74** containing the 2-amino moiety showed a pKa between 6.85 and 6.68, respectively from the pyrimidine system; our results argue that only a small fraction of the two compounds will be protonated at physiological pH. When fluorine (compound **74**) was introduced in the *ortho*-position, a decrease on the pKa of the vicinal pyrimidine took place, as suggested in previous reports.[36] When the 2-NH_2 entity was substituted by a hydrogen in compound **60**, the pKa of the pyrimidine underwent a major drop of ~3.25, underlying the 2-NH_2 entity as a contributor to increase basicity in the pyrimidine system (Table 2).

Two hydrogens of the pyridines in compounds **40** and **74** were followed by NMR. pKa from pyridine system in the three compounds varied from 4.1-4.3. We compared our results with *in silico* analysis utilizing Marvin Sketch software.[47] *In silico* profiles suggested protonation occurring on the endocyclic nitrogens of the pyrimidine system. Previous studies by Schiebel *et al*.[48] demonstrated protonation by nuclear diffraction, most likely to occur in an endocyclic nitrogen when exocyclic nitrogen is also available. The pKa's of ionizable moieties in the three compounds exhibited marked differences when compared to nicotine.

Drug-likeliness of analogues **40, 60** and **74** were determined *in silico* utilizing Marvin Sketch software (Table 2).[47] Clog P, hydrogen bond donors (HBD) and acceptors (HBA), and molecular weight (MW) of analyzed analogues are in the range of the "Lipinski's rule of 5".[49] The polar surface area (PSA) of 2-NH_2 analogues **40** and **74** is enhance when compared to compound **60**.

TABLE 2. pKa values for nicotine and compounds 40, 60 and 74 acquired by ^{1}H-NMR spectroscopy and physico-chemical properties.

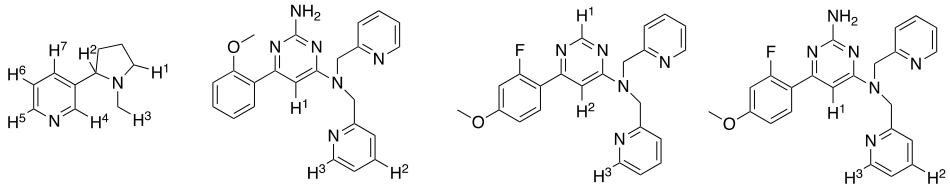

Nicotine **40** **60** **74**

COMPOUND	^{1}H-NMR pKa pyrimidine ring mean±SD	^{1}H-NMR pKa pyridine ring mean±SD	^{1}H-NMR pKa pyrrolidine ring mean±SD	*pKa pyrimidine ring	*pKa pyridine ring	*pKa pyrrolidine ring	*CLog P	*HBD	*HBA	*MW	*PSA
Nicotine	-	3.38±0.03	8.17±0.01	-	2.70	8.58	1.16	0	2	162.12	17.33
40	6.98	4.31±0.02	-	6.05 (-0.64)	4.39 (4.76)	-	3.65	1	7	398.19	90.05
60	~3.25	~4.14	-	3.53 (-1.62)	4.04 (4.53)	-	3.95	0	6	401.17	60.03
74	6.68	4.26±0.03	-	5.95 (-0.73)	4.39 (4.75)	-	3.80	1	7	416.18	90.05

**In silico* values calculated utilizing Marvin Sketch software.[47]

CONCLUSIONS

Herein we present the synthesis and pharmacological characterization of a non-canonical structural landscape of ligands for activation of α7 nAChRs that contains a pyrimidine center to which functionalization of positions 2, 4, 6 was made. Amino substitution in position 2 is important for enhancing activity of the series (Table 1), yet removal or substitution of the 2-amino motif does not eliminate sub-micromolar agonist responses (Table 1). For α7 agonist activity a required di(2-picolyl) amine substitution was made at the 4-position of the pyrimidine ring. The symmetry of the di-(2-picolyl) amine moiety is critical for activation of the α7 nAChR as seen in compound **75**. Functionalization of aromatic substitution in position 6 plays an important role in modulating the activity and selectivity.

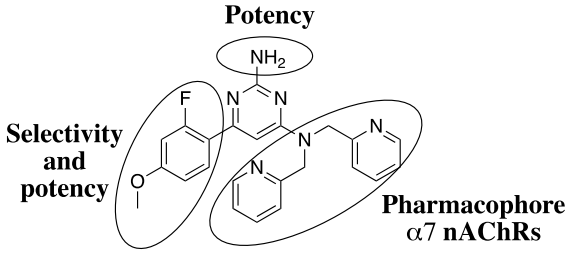

Electrophysiological measurements confirmed activation of α7 nAChR without the presence of PNU-120596, differing from the responses of silent agonists. Nevertheless, evaluation revealed stabilization of a desensitized PNU-sensitive closed state of α7 nAChR by the leads. These results, as well as the fact that the structures differ from classical agonists, opens the possibility of occupation of both the orthosteric and potential allosteric binding sites.[39] A more detailed electrophysiologic analysis beyond the scope of this article, directed to the chemical characterization of the series, is necessary to address these alternatives. Nevertheless, it is clear that this family of ligands differ from

other agonist classifications in terms of activation and desensitization.

Multiple endocyclic (pyrimidine and pyridine) and exocyclic nitrogens at the 2 and 4 positions are found in this landscape. Our titrations of chemical shifts in ^{1}H-NMR reveal that all of the nitrogens exist predominantly as neutral, non-ionized species at physiological pH values (Table 2). This contrasts with the classical nicotinic agonists with a separated two ring system, like nicotine, cytisine or epibatidine, one of which contains a strong base and the other a hydrogen bond donor or acceptor (Figure 1). It appears from the titration data that the 2-NH_2 group on the pyrimidine will contribute to incremental basicity in the pyrimidine system (Table 2). *In silico* analysis utilizing Marvin Sketch (Version 17.27.0) suggests that protonation may occur at endocyclic nitrogens (supporting information), as supported by previously published studies,[48-50] where calculation and nuclear diffraction identified endocyclic nitrogens in 2-aminopyridine and 2-aminopyrimidine as the more stable tautomer. Also, the lack of a dominant cationic species with a high pKa should facilitate disposition of these compounds at tissue target sites and the potential crossing of the blood-brain barrier to achieve CNS activities and perhaps possible side effects, physico-chemical properties of lead compounds are within threshold values for membrane permeation and oral bioavailability.[49-51]

A combination of a screen of moderate throughput, followed by detailed electrophysiologic measurements of currents, has enabled us to identify a series of non-canonical selective nAChR agonists. Certainly, this new library of compounds affords some interesting new possibilities and refreshes the concepts of ligand design for nAChRs.

EXPERIMENTAL SECTION

Materials. Epibatidine (Tocris, batch No. 14B/181649), PNU-120596 (Tocris, batch No. 3A/210007 and 3A/210046), MLA (Tocris, batch No: 20A/164724), 5-HT (Tocris, batch No: 2A/201353 and 2B/226517), Tropisetron (Tocris, batch No. 2B/214070), DHβE (Tocris, batch No. 11A/219484), FBS (Gibco, Lot: 834471), Glutamine (Gibco, Lot: 1894162). Reagents and solvents used for chemical synthesis and for buffer preparation were purchased from commercial sources in the highest purity available and used without further purification. All final compounds submitted for screening had a purity of 95% or higher (HPLC-MS), and chemical structures were confirmed by ^{1}H and ^{13}C NMR and HRMS (Supporting Information). For NMR assessment a 600MHz NMR spectrometer and a Bruker TopSpin 2.1.6 software was used. An Agilent 1260 liquid chromatography (LC) system coupled with a Thermo LCQdeca mass spectrometer was employed for LC-MS analysis. The electrospray ionization (ESI) source was operated under positive ion mode. An Agilent Zorbax SB-C18 column (ID 4.6 mm × length 150 mm, particle size 3.5 µm) was utilized for LC separation using water with 0.05 % TFA as mobile phase A and acetonitrile with 0.05 % TFA as mobile phase B. The LC flow rate was set at 1.0 mL/minute. The LC gradient setting is as followed: 0 minute: 5% mobile phase B, 12 minute: 95% mobile phase B, 14 minute: 95% mobile phase B, 15 minute: 5% mobile phase B, 20 minute: 5% mobile phase B. The total runtime was 20 minutes. High resolution mass spectrometry (HR-MS) data was acquired by using an Agilent 6230 time of flight mass spectrometer with Jetstream electrospray ionization source.

Syntheses.

6-chloro-2-(methylthio)-*N,N*-bis(pyridin-2ylmethyl)pyrimidin-4-amine (B-1). Di-(2-picolyl)amine (1.12 g, 5.63 mmol) was added to a solution 4,6-dichloro-2-(methylthio)pyrimidine (1.00 g, 5.01 mmol) and *N,N*-diisopropylethylamine (0.73 mL, 5.63 mmol) in DMF (8.0 mL) and the solution was stirred at 80 ºC for 3.5 hours (reaction monitored by TLC). The solvent was removed under reduced pressure, brine was added, and the mixture was extracted with ethyl acetate (3 x 40 mL). The organic layers were washed with brine, dried over anhydrous sodium sulfate and filtered. The filtrate was concentrated on a rotary evaporator, and the product was purified by column chromatography using silica gel (hexanes/EtOAc 3:2) or by crystallization. After purification a white solid was obtained in a 91% yield. ^{1}H NMR (600 MHz, Chloroform-*d*) δ 2.37 (s, 3H), 4.74 (s, 2H), 5.14 (s, 2H), 6.22 (s, 1H), 7.26 – 7.12 (m, 4H), 7.64 (td, *J* = 7.7, 1.6 Hz, 2H), 8.54 (s, 2H). HR-ESI-TOFMS: $[C_{17}H_{17}ClN_5S]^+$ 358.0885

6-chloro-*N,N*-bis(pyridin-2-ylmethyl)pyrimidin-4-amine (B-2). Di-(2-picolyl)amine (1.45 mL, 8.0 mmol) was added to a solution of 4,6-dichloropyrimidine (1.00 g, 6.70 mmol) and *N,N*-diisopropylethylamine (1.40 mL, 8.00 mmol) in DMF (9.0 mL) and the solution was stirred at 80 ºC for 1.5 hours (reaction monitored by TLC). The solvent was removed under reduced pressure, brine was added and the mixture was extracted with ethyl acetate (3 x 40 mL). The organic layers were washed with brine, dried over anhydrous sodium sulfate and filtered. The filtrate was concentrated on a rotary evaporator, and the product was purified by column chromatography using silica gel and hexanes-EtOAc (1:3). After purification a white solid was obtained in a 64% yield. ^{1}H NMR (600 MHz, Chloroform-*d*) δ 4.77 (s, 2H), 5.12 (s, 2H), 6.54 (s, 1H), 7.30 – 7.11 (m, 4H), 7.65 (td, *J* = 7.7, 1.7 Hz, 2H), 8.44 (s, 1H), 8.57 (s, 2H). ^{13}C-APT NMR (151 MHz, Chloroform- *d*) δ 53.7 (CH_2), 102.2 (CH), 102.2 (CH), 122.9 (CH), 137.2 (CH), 158.3 (CH), 160.0 (C), 160.3 (C), 163.4 (C). HR-ESI-TOFMS: $[C_{16}H_{15}ClN_5]^+$ 312.1007

6-chloro-*N,N*-bis(pyridin-2-ylmethyl)-2-(trifluoromethyl)pyrimidin-4-amine (B-3). Di-(2-picolyl)amine (0.22 mL, 1.20 mmol) was added to a solution of 4,6-dichloro-2-(trifluoromethyl)pyrimidine (0.22 g, 1.00 mmol) and *N,N*-diisopropylethylamine (0.21 mL, 1.20 mmol) in DMF (1.5 mL) and the solution was stirred at 80 ºC for 3.5 hours (reaction monitored by TLC). The solvent was removed under reduced pressure, brine was added and the mixture was extracted with ethyl acetate (3 x 20 mL). The organic layers were washed with brine, dried over anhydrous sodium sulfate and filtered. The filtrate was concentrated on a rotary evaporator, and the product was purified by column chromatography using silica gel (hexanes/EtOAc 7:3). After purification a white solid was obtained in a 93% yield. ^{1}H NMR (600 MHz, Chloroform-*d*) δ 4.87 (s, 2H), 5.15 (s, 2H), 6.66 (s, 1H), 7.17 (d, *J* = 7.1 Hz, 1H), 7.26 – 7.19 (m, 2H), 7.42 (d, *J* = 7.1 Hz, 1H), 7.70 – 7.62 (m, 2H), 8.57 (d, *J* = 38.8 Hz, 2H). ^{13}C-APT NMR (151 MHz, Chloroform-*d*) δ 55.2 (CH_2), 104.0 (CH), 116.5-121.95 (q, $^1J_{C-F}$= 276.3 Hz, CF_3), 121.3 (CH), 123.1 (CH), 123.2 (CH), 123.5 (CH), 149.6 (CH), 150.4 (CH), 155. 3 (C),

156.5-155.7 (q, $^2J_{C\text{-}F}$ = 36.96 Hz, C), 156.4 (C), 160.8 (C), 163.6 (C). HR-ESI-TOFMS: $[C_{17}H_{14}ClF_3N_5]^+$ 380.0879. HPLC: 99% pure.

***N*-benzyl-1-(pyridin-2-yl)methanamine (B-4).** To a solution of benzylamine (0.54 g, 5.00 mmol) in 4 mL of ethanol, pyridine-2-carboxaldehyde (0.54 g, 5.00 mmol) in 4.0 mL of ethanol was added. The solution was stirred overnight and boiled gently for 30 min. $NaBH_4$ (0.25 g, 6.50 mmol) was slowly added at 0 ºC. After 2 hours, 7 mL of H_2O was slowly added following by addition of 20 mL of a saturated solution of NH_4Cl, bring to pH 7 the solution, the mixture was extracted with ethyl acetate (3 x 30 mL). The filtrate was concentrated under reduced pressure and the crude oil was purified. Oxalic acid was added (0.64 g, 5.04 mmol) in 15 mL of ethanol. The salt was filtered and dissolved in 20 mL of H_2O following by addition of NaOH (30%), extractions with EtOAc was made. The organic solvent was removed and B-5 (oil) was isolated in a 67% yield. ^{1}H NMR (600 MHz, Chloroform-*d*) δ 2.52 (s, 1H), 3.86 (s, 2H), 3.94 (s, 2H), 7.20 – 7.14 (m, 1H), 7.26 (t, *J* = 7.2 Hz, 1H), 7.34 (td, *J* = 8.4, 7.9, 2.0 Hz, 3H), 7.38 (d, *J* = 7.5 Hz, 2H), 7.65 (td, *J* = 7.6, 1.8 Hz, 1H), 8.57 (ddd, *J* = 4.8, 1.6, 0.8 Hz, 1H). HR- ESI-TOFMS: $[C_{13}H_{15}N_2]^+$ 199.1223

***N*^{4}-benzyl-6-chloro-*N*^{4}-(pyridin-2-ylmethyl)pyrimidine-2,4-diamine (B-5).** *N*-benzyl-1-(pyridin-2-yl)methanamine (0.50 g, 2.50 mmol) was added to a solution of 2-amino-4,6-dichloropyrimidine (0.37 g, 2.20 mmol) and *N,N*-diisopropylethylamine (0.44 mL, 2.50 mmol) in DMF (3.4 mL) and the solution was stirred at 80 ºC overnight. The solvent was removed under reduced pressure, brine was added and the mixture was extracted with ethyl acetate (3 x 40 mL). The organic layers were washed with brine, dried over anhydrous magnesium sulfate, and filtered. The filtrate was concentrated on the rotary evaporator, and the product was purified by column chromatography using silica gel (EtOAc/MeOH 9:1). After purification a white solid was obtained in a 36% yield. ^{1}H NMR (600 MHz, Chloroform-*d*) δ 4.96 (s, 6H), 5.94 (s, 1H), 7.20 (dd, *J* = 13.8, 6.6 Hz, 3H), 7.28 (t, *J* = 7.2 Hz, 2H), 7.33 (t, *J* = 7.3 Hz, 2H), 7.64 (td, *J* = 7.7, 1.8 Hz, 1H), 8.57 (d, *J* = 4.3 Hz, 1H). ^{13}C-APT NMR (151 MHz, Chloroform-*d*) δ 52.7 (CH_2), 92.8 (CH), 110.4 (CH), 120.2 (CH), 122.6 (CH), 127.7 (CH), 129.0 (CH), 137.1 (CH), 149.8 (CH), 160.6 (C), 162.3 (C), 164.4(C). HR-ESI-TOFMS: $[C_{17}H_{17}ClN_5]^+$ 326.1165.

6-chloro-*N*^{4},*N*^{4}-bis(pyridin-2-ylmethyl)pyrimidine-2,4-diamine (B-21). B-21 was synthesized as previously describe.[23] Di-(2-picolyl)amine (0.44 mL, 2.20 mmol) was added to a solution of 2-amino-4,6-dichloropyrimidine (0.33 g, 2.00 mmol) and *N,N*-diisopropylethylamine (0.38 mL, 2.20 mmol) in DMF (3.0 mL) and the solution was stirred at 80 ºC for 3.5 hours (reaction monitored by TLC). The solvent was removed under reduced pressure, brine was added and the mixture was extracted with ethyl acetate (3 x 20 mL). The organic layers were washed with brine, dried over anhydrous sodium sulfate and filtered. The filtrate was concentrated on a rotary evaporator, and the product was purified by column chromatography using silica gel (hexanes/EtOAc 7:3) or by crystallization (the compound crystalized using ethyl acetate as solvent). After purification a white solid was obtained in a 63% yield. ^{1}H NMR (600 MHz, Chloroform-*d*) δ 4.74 (bs, 2H), 4.99 (s, 4H), 5.94 (s, 1H), 7.12-7.23 (m, 4H), 7.55–7.69 (m, 2H), 8.52–8.57 (d, *J* = 4.0 Hz, 2H). ^{13}C-APT NMR (150 MHz, Chloroform-*d*) δ 53.2 (CH_2), 92.7 (CH), 122.4 (CH), 136.8 (CH), 149.6 (CH), 160.4 (C), 162.1 (C), 164.1 (C), 170.1 (C). HR-ESI-MS: $[C_{16}H_{16}N_6Cl]^+$ 327.1124.

6-(2-methoxyphenyl)-2-(methylthio)-*N*,*N*-bis(pyridin-2-ylmethyl)pyrimidin-4-amine(56). 2-Methoxyphenyl boronic acid (0.59 g, 3.91 mmol) was added to a solution of 6-chloro-2-(methylthio)-*N,N*-bis(pyridin-2-ylmethyl)pyrimidin-4-amine (**B-1**) (1.00 g, 2.80 mmol) in DMA (22 mL), 2 M aqueous potassium carbonate (4.19 mL) was added following the addition of Pd(dppf)Cl_2 (0.20 g, 0.28 mmol). The resulting mixture was stirred in a capped glass vial at 149 ºC overnight. The solvent was removed under reduced pressure, brine was added and the mixture was extracted with ethyl acetate (3 x 50 mL). The organic layers were dried over anhydrous magnesium sulfate, and filtered. The filtrate was concentrated under reduced pressure and the crude product was filtrate through silica gel and recrystallized in ethyl acetate to give white solid in a 53% yield. ^{1}H NMR (600 MHz, Chloroform-*d*) δ 2.47 (s, 3H), 3.61 (s, 3H), 4.85 (s, 2H) , 5.22 (s, 2H), 6.85 (s, 1H), 6.88 (d, *J* = 8.3 Hz, 1H), 7.02 (t, *J* = 7.5 Hz, 1H), 7.20 (dd, *J* = 7.1, 5.1 Hz, 2H), 7.34 (t, *J* = 7.8 Hz, 2H), 7.65 (t, *J* = 7.6 Hz, 2H), 7.93 (dd, *J* = 7.7, 1.7 Hz, 1H), 8.57 (s, 2H). ^{13}C-APT NMR (151 MHz, Chloroform-*d*) δ 14.2 (CH_3), 53.6 (CH_2), 55.3 (CH_3), 99.5 (CH), 111.3 (CH), 114.2 (C), 120.0 (CH), 120.9 (CH), 122.3 (CH), 126.9 (C), 130.8 (CH), 130.9 (CH), 136.9 (CH), 157.6 (C), 161.5 (C), 162.0 (C), 170.63 (C). HR-ESI-TOFMS: $[C_{24}H_{24}N_5OS]^+$ 430.1692. HPLC: 99% pure.

2-(methylthio)-*N*,*N*-bis(pyridin-2-ylmethyl)-6-(thiophen-3-yl)pyrimidin-4-amine(57). 3-Thienylboronic acid (0.04 g, 0.30 mmol) was added to a solution of 6-chloro-2-(methylthio)-*N,N*-bis(pyridin-2-ylmethyl)pyrimidin-4-amine (**B-1**) (0.10 g, 0.3 mmol) in DMA (2.0 mL), 2 M aqueous potassium carbonate (0.3 mL) was added following the addition of Pd(dppf)Cl_2 (22 mg, 0.030 mmol). The resulting mixture was stirred in a capped glass vial at 149ºC overnight. The solvent was removed under reduced pressure, brine was added and the mixture was extracted with ethyl acetate (3 x 50 mL). The organic layers were dried over anhydrous magnesium sulfate, and filtered. The filtrate was concentrated under reduced pressure and the product was isolated by column chromatography on silica gel using Hex/EtOAc gradient (pale solid, 40% yield). ^{1}H NMR (600 MHz, Chloroform-*d*) δ 2.47 (s, 3H), 4.86 (s, 2H), 5.18 (s, 2H), 6.47 (s, 1H), 7.19 (dd, *J* = 7.0, 5.2 Hz, 3H), 7.36 – 7.26 (m, 2H), 7.49 – 7.44 (m, 1H), 7.63 (t, *J* = 7.2 Hz, 2H), 7.94 (d, *J* = 2.1 Hz, 1H), 8.57 (s, 2H). ^{13}C-APT NMR (151 MHz, Chloroform-*d*) δ 14.2 (CH_3), 53.7 (CH_2), 94.2 (CH), 122.5 (CH), 125.9 (CH), 126.0 (CH), 126.2 (CH), 127.3 (CH), 127.8 (CH), 136.9 (CH), 140.7 (C), 159.1 (C), 162.4 (C), 171.3 (C). HR-ESI-TOFMS: $[C_{21}H_{20}N_5S_2]^+$ 406.1152 HPLC: 95% pure.

6-(3,4-dimethoxyphenyl)-*N*^{4},*N*^{4}-bis(pyridin-2ylmethyl) pyrimidine-2,4-diamine (58). 2-Methoxyphenylboronic acid (0.05 g, 0.30 mmol) was added to a solution of 6-chloro-*N,N*-bis(pyridin-2-ylmethyl)pyrimidin-4-amine (**B-2**) (0.075 g, 0.24 mmol) in DMA (2.0 mL), 2 M aqueous potassium carbonate (0.25 mL) was added following the addition of Pd(dppf)Cl_2 (17 mg, 0.024 mmol). The resulting mixture was stirred in a capped glass vial at 149 ºC overnight. DMA was removed under reduced pressure, brine

was added and the mixture was extracted with ethyl acetate (3 x 30 mL). The organic layers were dried over anhydrous magnesium sulfate, and filtered. The filtrate was concentrated under reduced pressure and the crude product was purified by column chromatography on silica gel with CH_3Cl/MeOH/NH_4OH 100/1.2/0.2 to give the product as a white solid in a 49% yield. ^{1}H NMR (600 MHz, Chloroform-*d*) δ 3.62 (s, 3H), 4.95 (s, 3H), 6.92 – 6.87 (m, 1H), 7.10 (d, *J* = 1.1 Hz, 1H), 7.04 (t, *J* = 8.0 Hz, 1H), 7.20 (dd, *J* = 7.0, 5.3 Hz, 2H), 7.40 – 7.28 (m, 2H), 7.65 (td, *J* = 7.7, 1.7 Hz, 2H), 7.86 (dd, *J* = 7.7, 1.8 Hz, 1H), 8.58 (d, *J* = 4.4 Hz, 2H), 8.78 (s, 1H). ^{13}C NMR (151 MHz, Chloroform-*d*) δ 53.5 (CH_2), 55.4 (CH_3), 103.8 (CH), 111.4 (CH), 121.0 (CH), 122.5 (CH), 127.1 (C), 129.1 (CH), 130.8 (CH), 130.9 (CH), 137.0 (CH), 149.7 (CH), 156.4 (C), 157.4 (C), 158.2 (CH), 161.6 (C), 162.4 (C). HR-ESI-TOFMS: $[C_{23}H_{22}N_5O]^+$ 384.1820 HPLC: 99% pure.

***N*,*N*-bis(pyridin-2-ylmethyl)-6-(thiophen-3-yl)pyrimidin-4-amine (59).** 3-Thienylboronic acid (0.08 g, 0.62 mmol) was added to a solution of 6-chloro-*N,N*-bis(pyridin-2-ylmethyl)pyrimidin-4-amine (**B-2**) (0.15 g, 0.62 mmol) in DMA (3.0 mL), 2 M aqueous potassium carbonate (0.72 mL) was added following the addition of Pd(dppf)Cl_2 (35 mg, 0.05 mmol). The resulting mixture was stirred in a capped glass vial at 149 °C overnight. DMA was removed under reduced pressure, brine was added and the mixture was extracted with ethyl acetate (3 x 30 mL). The organic layers were dried over anhydrous magnesium sulfate, and filtered. The compound was purified using silica gel columns Hex/EtAcO 1:4 to give a white solid in a 74% yield. ^{1}H NMR (600 MHz, Chloroform-*d*) δ 8.70 – 8.67 (m, 1H), 8.59 (d, *J* = 4.4 Hz, 2H), 7.96 – 7.93 (m, 1H), 7.64 (td, *J* = 7.7, 1.7 Hz, 2H), 7.48 (dd, *J* = 5.1, 1.2 Hz, 1H), 7.34 (dd, *J* = 5.1, 3.0 Hz, 1H), 7.25 (s, 1H), 7.20 (dd, *J* = 7.1, 5.2 Hz, 3H), 6.78 (s, 1H), 5.08 (d, *J* = 57.2 Hz, 4H). ^{13}C-APT NMR (151 MHz, Chloroform-*d*) δ 53.8 (CH_2), 95.8(CH), 122.7 (CH), 125.9 (CH), 126.1(CH), 126.7(CH), 137.2 (CH), 141.0 (C), 149.9 (C), 158.7 (CH), 159.1 (C), 163.0 (C). HR-ESI-TOFMS: $[C_{20}H_{18}N_5S]^+$ 360.1279 HPLC: 98% pure.

6-(2-fluoro-4-methoxyphenyl)-*N*,*N*-bis(pyridin-2-ylmethyl)pyrimidin-4-amine (60). 2-fluoro-4-methoxybenzene boronic acid (0.12 g, 0.67 mmol) was added to a solution of 6-chloro-*N,N*-bis(pyridin-2-ylmethyl)pyrimidin-4-amine (**B-2**) (0.15 g, 0.48 mmol) in THF (3.5 mL), 2 M aqueous sodium carbonate (0.72 mL) was added following the addition of $Pd(PPh_3)_4$ (0.06 g, 0.048 mmol). The resulting mixture was vigorously stirred in reflux for 6 hours. THF was removed under reduced pressure, brine was added and the mixture was extracted with ethyl acetate (3 x 20 mL). The organic layers were dried over anhydrous magnesium sulfate, and filtered. The crude was purified using a biotage® ZIP™ 10 g Si cartridge Hex/EtOAc gradients. White solid in a 68% yield. ^{1}H NMR (600 MHz, Chloroform-*d*) δ 8.74 (s, 1H), 8.59 (d, *J* = 4.3 Hz, 2H), 8.00 (t, *J* = 8.9 Hz, 1H), 7.65 (td, *J* = 7.7, 1.5 Hz, 2H), 7.26 (s, 2H), 7.20 (dd, *J* = 7.0, 5.3 Hz, 2H), 6.97 (s, 1H), 6.79 (dd, *J* = 8.8, 2.5 Hz, 1H), 6.65 – 6.59 (m, 1H), 5.14 (s, 4H), 3.83 (s, 3H).^{13}C-DEPTQ NMR (151 MHz, Chloroform-*d*) δ 53.6 (CH_2), 55.8 (CH_3), 102.1 –102.3 (d, ^2J=26.84 Hz, CH), 102.2 (CH), 102.4 – 102.5 (d, ^4J = 11.54 Hz, CH), 110.5 – 110.6 (d, ^4J = 2.86 Hz, CH), 118.4 – 118.5 (d, ^2J = 10.74 Hz, C), 122.6 (CH), 131.5 – 131.6 (d, ^3J = 4.58 Hz, CH), 137.0 (CH), 149.8 (CH), 158.4 (CH), 159.0 (d, ^3J = 3.08 Hz, C), 160.3 (C), 161.1 – 162.8 (d, ^1J = 251.79 Hz, C), 162.2 – 162.3 (d, ^3J = 11.53Hz, C), 162.63 (C). HR-ESI-TOFMS: $[C_{23}H_{21}FN_5O]^+$ 402.1720 HPLC: 95% pure.

6-(2-fluorophenyl)-*N*,*N*-bis(pyridin-2-ylmethyl)pyrimidin-4-amine (61). 2-fluorophenyl boronic acid (0.13 g, 0.90 mmol) was added to a solution of 6-chloro-*N,N*-bis(pyridin-2-ylmethyl)pyrimidin-4-amine (**B-2**) (0.2 g, 0.64 mmol) in THF (4.6 mL), 2 M aqueous sodium carbonate (0.96 mL) was added following the addition of $Pd(PPh_3)_4$ (0.07 g, 0.06 mmol). The resulting mixture was vigorously stirred in reflux overnight. THF was removed under reduced pressure, brine was added and the mixture was extracted with ethyl acetate (3 x 20 mL). The organic layers were dried over anhydrous magnesium sulfate, and filtered. The crude was purified using a biotage® ZIP™ 10g Si cartridge and Hex/EtOAc gradients. White solid in a 81% yield. ^{1}H NMR (600 MHz, Chloroform-*d*) δ 8.78 (s, 1H), 8.59 (d, *J* = 4.5 Hz, 2H), 7.99 (td, *J* = 7.8, 1.5 Hz, 1H), 7.65 (t, *J* = 7.6 Hz, 2H), 7.37 (q, *J* = 7.5, 7.0 Hz, 1H), 7.30 – 7.17 (m, 5H), 7.09 (dd, *J* = 11.4, 8.3 Hz, 1H), 7.01 (s, 1H), 5.05 (s, 4H). ^{13}C-DEPTQ NMR (151 MHz, Chloroform-*d*) δ 53.6 (CH_2), 103.3 – 103.4 (d, ^4J = 10.17 Hz, CH), 116.3 – 116.6 (d, ^2J = 22.88 Hz, CH), 122.6 (CH), 124.6 (d, ^4J = 3.66Hz, CH), 126.1 – 126.2 (d, ^2J = 10.68 Hz, C), 130.8 – 130.9 (d, ^3J= 2.6 Hz, CH), 131.4 –131.5 (d, ^3J = 8.6 Hz, CH), 137.0 (CH), 149.8 (CH), 158.5 (CH), 159.1 – 159.2 (d, ^3J = 2.44 Hz, C), 160.1 – 161.7 (d, ^1J = 251.56 Hz, C), 162.6 (C). HR-ESI-TOFMS: $[C_{22}H_{19}FN_5]^+$ 372.1619 HPLC: 99% pure.

6-(2-methoxyphenyl)-*N*,*N*-bis(pyridin2-ylmethyl)-2(trifluoromethyl) pyrimidin-4-amine(62). 2-Methoxyphenylboronic acid (0.05 g, 0.34 mmol) was added to a solution of 6-chloro-*N,N*-bis(pyridin-2-ylmethyl)-2-(trifluoromethyl)pyrimidin-4-amine (**B-3**) (0.10 g, 0.34 mmol) in DMA (2.0 mL), 2 M aqueous potassium carbonate (0.20 mL) was added following the addition of Pd(dppf)Cl_2 (19 mg, 0.030 mmol). The resulting mixture was stirred in a capped glass vial at 149 °C overnight. DMA was removed under reduced pressure, brine was added and the mixture was extracted with ethyl acetate (3 x 30 mL). The organic layers were dried over anhydrous magnesium sulfate, and filtered. The filtrate was concentrated under reduced pressure and the crude product was purified by column chromatography on silica gel with Hex/EtOAc 1:4 to give the product as a white solid in a 38% yield. ^{1}H NMR (600 MHz, Chloroform-*d*) δ 3.61 (s, 3H), 4.92 (s, 2H), 5.23 (s, 2H), 6.90 (d, *J* = 8.2 Hz, 1H), 7.05 (t, *J* = 7.5 Hz, 1H), 7.21 (s, 3H), 7.25 (s, 1H), 7.40 – 7.33 (m, 1H), 7.52 (s, 1H), 7.67 (s, 2H), 8.02 – 7.98 (m, 1H), 8.58 (d, *J* = 25.7 Hz, 2H). ^{13}C-APT NMR (151 MHz, Chloroform-*d*) δ 54.26 (CH_2), 55.6 (CH_3), 105.3 (CH), 105.5 (CH), 111.6 (CH), 118.4 –121.8 (q, $^1J_{C\text{-}F}$ = 276.3 Hz, CF_3), 121.3 (CH), 122.8 (CH), 123.0 (CH), 126.1 (C), 131.3 (CH), 131.6 (C), 137.1(CH), 155.6 – 156.3 (q, $^2J_{C\text{-}F}$ = 36.2 Hz, C) 156.2 (CH), 157.8 (C), 161.9 (C), 162.9 (C). HR-ESI-TOFMS: $[C_{24}H_{21}F_3N_5O]^+$ 452.1689 HPLC: 95% pure.

***N*,*N*-bis(pyridin-2-ylmethyl)-6-(thiophen-3-yl)-2-(trifluoromethyl)pyrimidin-4-amine (63).** 3-Thienylboronic acid (0.07 g, 0.51 mmol) was added to a solution of 6-chloro-N,N-bis(pyridin-2-ylmethyl)-2-(trifluoromethyl)pyrimidin-4-amine (**B-3**) (0.15 g, 0.40 mmol) in DMA (2.6 mL), 2 M aqueous potassium carbonate (0.59 mL) was added following the addition of Pd(dppf)Cl_2 (29 mg, 0.040 mmol). The resulting mixture was stirred in a

capped glass vial at 149 °C for 3.5 hours. DMA was removed under reduced pressure, brine was added and the mixture was extracted with ethyl acetate (3 x 20 mL). The organic layers were dried over anhydrous magnesium sulfate, and filtered. Purification, using column chromatography on silica gel (hexanes/EtOAc 1:4), afforded the product (pale solid) in a 95% yield. ^{1}H NMR (600 MHz, Chloroform-*d*) δ 8.64 – 8.50 (m, 2H), 8.03 (dd, *J* = 3.0, 1.1 Hz, 1H), 7.65 (s, 2H), 7.48 (dd, *J* = 5.1, 1.1 Hz, 2H), 7.34 (dd, *J* = 5.1, 3.1 Hz, 1H), 7.21 (dd, *J* = 7.1, 5.2 Hz, 3H), 6.84 (s, 1H), 5.22 (s, 2H), 4.94 (s, 2H). ^{13}C-DEPTQ NMR (151 MHz, Chloroform-*d*) δ 54.0 (CH_2), 99.6 (CH), 116.9 – 122.4 (C, q, $^1J_{C\text{-}F}$ = 276.1 Hz, CF_3), 122.7 (CH), 125.7 (CH), 126.5 (CH), 126.8 (CH), 128.5 (CH), 136.9 (CH), 139.7 (C), 145.37 (CH), 155.8 – 156.5 (C, q $^2J_{C\text{-}F}$ = 35.5 Hz, CF_3)159.5 (C), 163.1 (C). HR-ESI-TOFMS $[C_{21}H_{17}F_3N_5S]^+$ 428.1152 HPLC: 99% pure.

6-(2-methoxyphenyl)-2-(methylsulfonyl)-*N*,*N*-bis(pyridin-2 ylmethyl)pyrimidin-4-amine(64). 56 (0.30 g, 0.70 mmol) was dissolved in (1.5 mL) DCM, following by slow addition of *m*-CPBA (0.25 g, 1.50 mmol) at 0 °C. After 3 hours, saturated solution of $Na_2S_2O_3$ was added and the mixture was extracted with ethyl acetate (2 x 40 mL). The organic layers were washed with saturated solution of $NaHCO_3$ and the mixture was extracted with ethyl acetate (3 x 40 mL). The organic layers were dried over anhydrous magnesium sulfate, and filtered. The filtrate was concentrated under reduced pressure and the crude product was purified by column chromatography on silica gel with Hex/EtOAc 1:4 to give white solid in a 31% yield. ^{1}H NMR (600 MHz, Chloroform-*d*) δ 8.59 (d, *J* = 46.9 Hz, 2H), 8.07 (dd, *J* = 7.8, 1.9 Hz, 1H), 7.68 (s, 2H), 7.56 (s, 1H), 7.42 – 7.38 (m, 1H), 7.37 (s, 1H), 7.26 – 7.16 (m, 3H), 7.06 (t, *J* = 7.6 Hz, 1H), 6.92 (d, *J* = 8.3 Hz, 1H), 5.24 (s, 2H), 4.96 (s, 2H), 3.64 (s, 3H), 3.29 (s, 3H). ^{13}C-APT NMR (151 MHz, Chloroform-*d*) δ 38.9 (CH_3), 54.5 (CH_2), 55.5 (CH_3), 105.9 (CH), 111.5 (CH), 120.7 (CH), 121.2 (CH), 123.3 (CH), 125.2 (C), 131.3 (CH), 131.9 (CH), 137.2 (CH), 149.9 (CH), 156.3 (C), 158.0 (C), 161.7(C), 163.1 (C), 165.0 (C). HR-ESI-TOFMS: $[C_{24}H_{24}N_5O_3S]^+$ 462.1592 HPLC: 95% pure.

6-(2-methoxyphenyl)-2(methylsulfinyl)-*N*,*N*-bis(pyridin-2-ylmethyl)pyrimidin-4-amine(65). 56 (0.10 g, 0.23 mmol) was dissolved in (1.0 mL) DCM, followed by slow addition of *m*-CPBA (0.04g, 0.23 mmol) at 0 °C. After 3 hours, a saturated solution of $Na_2S_2O_3$ was added and the mixture was extracted with ethyl acetate (2 x 20 mL). The organic layers were washed with saturated solution of $NaHCO_3$ and the mixture was extracted with ethyl acetate (3 x 20 mL). The organic layers were dried over anhydrous magnesium sulfate, and filtered. The filtrate was concentrated under reduced pressure and the crude product was purified by column chromatography on silica gel with EtOAc/MeOH 9:1 to give white solid in a 79% yield. ^{1}H NMR (600 MHz, Chloroform-*d*) δ 2.88 (s, 3H) 3.64 (s, 3H), 4.92 (s, 2H), 5.27 (d, *J* = 27.6 Hz, 2H), 6.90 (d, *J* = 8.2 Hz, 1H), 7.04 (t, *J* = 8.0 Hz, 1H), 7.21 (s, 2H), 7.23 (s, 2H), 7.39 – 7.34 (m, 1H), 7.53 (s, 1H), 7.67 (t, *J* = 7.1 Hz, 2H), 8.06 (dd, *J* = 7.8, 1.8 Hz, 1H), 8.61 (s, 2H).^{13}C-APT NMR (151 MHz, Chloroform-*d*) δ 39.9(CH_3), 54.0 (CH_2), 55.5 (CH_3), 104.2 (CH), 111.5 (CH), 121.2 (CH), 122.7 (CH), 125.8 (C), 131.4 (CH), 131.7 (CH), 137.1 (CH), 157.9 (C), 162.0 (C), 163.2 (C), 172.0 (C). HR-ESI-TOFMS $[C_{24}H_{24}N_5O_2S]^+$ 446.1645 HPLC: 99% pure.

6-morpholino-*N*,*N*-bis(pyridin-2-ylmethyl)pyrimidin-4-amine (66). To a solution of 6-chloro-*N*,*N*-bis(pyridin-2-ylmethyl)pyrimidin-4-amine (**B-2**) (0.15 g, 0.48 mmol) in 2-propanol (0.96 mL) morpholine (0.05 g, 0.57 mmol) and *N*,*N*-diisopropylethylamine (0.12 g, 0.95 mmol) was added. The resulting mixture was stirred in microwave sealed vial for 20 min at 160 °C. Solvent was removed at reduced pressure, brine was added and the mixture was extracted with ethyl acetate. The organic layers were dried over anhydrous magnesium sulfate, and filtered. The filtrate was concentrated under reduced pressure. The crude was purified using a biotage® ZIP™ 10 g Si cartridge and Hex/EtOAc gradients. Compound was isolated with EtOAc 100%. Pale powder in a 58% yield. ^{1}H NMR (600 MHz, Chloroform-*d*) δ 8.56 (d, *J* = 4.7 Hz, 2H), 8.29 (s, 1H), 7.64 (td, *J* = 7.7, 1.6 Hz, 2H), 7.24 (d, *J* = 7.8 Hz, 2H), 7.19 (dd, *J* = 7.2, 5.1 Hz, 2H), 5.57 (s, 1H), 4.96 (s, 4H), 3.74–3.69 (m, 4H), 3.46–3.40 (m, 4H). ^{13}C-DEPTQ NMR (151 MHz, Chloroform-*d*) δ 44.6 (CH_2), 53.9 (CH_2), 66.7 (CH_2), 81.9 (CH), 121.6 (CH), 122.5 (CH), 137.1 (CH), 149.6 (CH), 157.7 (CH), 158.0(C), 163.0 (C), 163.5 (C). HR-ESI-TOFMS $[C_{20}H_{23}N_6O]^+$ 363.1930 HPLC: 99% pure.

6-(2-methoxypyridin-3-yl)-N^4,N^4-bis(pyridin-2-ylmethyl)pyrimidine-2,4-diamine (67). 2-methoxy-3-pyridinephenyl boronic acid (0.11 g, 0.73 mmol) was added to a solution of 6-chloro-N^4,N^4-bis(pyridin-2-ylmethyl)pyrimidine-2,4-diamine (**B-21**) (0.20 g, 0.60 mmol) in DMA (5.0 mL), 2 M aqueous potassium carbonate (0.92 mL) was added following the addition of $Pd(dppf)Cl_2$ (45 mg, 0.06 mmol). The resulting mixture was stirred in a capped glass vial at 149 °C for 18 hours. DMA was removed under reduced pressure, brine was added and the mixture was extracted with ethyl acetate (3 x 20 mL). The organic layers were dried over anhydrous magnesium sulfate, and filtered. The filtrate was concentrated under reduced pressure and the crude product was isolated by silica gel column, the compound came out with EtOAc/MeOH 9:1, pale powder, 73% yield. ^{1}H NMR (600 MHz, Chloroform-*d*) δ 8.6 (d, *J* = 4.4 Hz, 2H), 8.2 (d, *J* = 9.4 Hz, 1H), 8.2 (d, *J* = 6.9 Hz, 1H), 7.7 (t, *J* = 8.5 Hz, 2H), 7.3 (s, 2H), 7.2 (dd, *J* = 7.1, 5.1 Hz, 2H), 7.0 (dd, *J* = 7.4, 4.9 Hz, 1H), 6.7 (s, 1H), 5.1 (s, 3H), 4.8 (s, 2H), 3.8 (s, 3H).^{13}C-DEPTQ NMR (151 MHz, Chloroform-*d*) δ 53.5 (CH_3), 95.4 (CH), 117.2 (CH), 122.1 (C), 122.3 (CH), 136.9 (CH), 139.1 (CH), 147.4 (CH), 161.1 (C), 161.4 (C), 162.3 (C), 162.8 (C), 163.9 (C).HR-ESI-TOFMS: $[C_{22}H_{22}N_7O]^+$ 400.1883 HPLC: 98% pure.

6-(2,6-dimethoxyphenyl)-N^4,N^4-bis(pyridin-2-ylmethyl)pyrimidine-2,4-diamine (68). 2,6-dimethoxyphenylboronic acid (0.17 g, 0.92 mmol) was added to a solution of 6-chloro-N^4,N^4-bis(pyridin-2-ylmethyl)pyrimidine-2,4-diamine (**B-21**) (0.20 g, 0.61 mmol) in DMA (3.8 mL), 2 M aqueous potassium carbonate (0.92 mL) was added following the addition of $Pd(dppf)Cl_2$ (45 mg, 0.06 mmol). The resulting mixture was stirred in a capped glass vial at 149 °C for 24 hours. DMA was removed under reduced pressure, brine was added and the mixture was extracted with ethyl acetate (3 x 30 mL). The organic layers were dried over anhydrous magnesium sulfate, and filtered. The crude was purified using a biotage® ZIP™ 10 g Si cartridge and Hex/EtOAc gradients. Pale powder, 42% yield. ^{1}H NMR (600 MHz, Chloroform-*d*) δ 8.5 (d, *J* = 4.5 Hz, 2H), 7.7 (t, *J* = 7.2 Hz, 2H), 7.3 (s, 2H), 7.2 (t, *J* = 8.4 Hz, 1H), 7.19 – 7.15 (m, 2H), 6.6 (d, *J* = 8.4 Hz, 2H), 5.9 (s,

1H), 4.9 (s, 4H), 4.8 (s, 2H), 3.7 (s, 6H).^{13}C- DEPTQ NMR (151 MHz, Chloroform-*d*) δ 56.1 (CH_3), 83.9 (C), 96.9 (CH), 104.4 (CH), 107.0 (CH), 122.2 (CH), 129.8 (CH), 132.9 (CH), 136.8 (CH), 157.9 (C), 163.5 (C). HR-ESI-TOFMS: $[C_{24}H_{25}N_6O_2]^+$ 429.2029 HPLC: 99% pure.

6-(4-fluoro-2-methoxyphenyl)-*N*^{4},*N*^{4}-bis(pyridin-2-ylmethyl)pyrimidine-2,4-diamine (69). 4-fluoro-2-methoxyphenyl boronic acid (0.104 g, 0.6 mmol) was added to a solution of 6-chloro-*N*^{4},*N*^{4}-bis(pyridin-2-ylmethyl)pyrimidine-2,4-diamine (**B-21**) (0.15 g, 0.45 mmol) in DMA (3.0 mL), 2 M aqueous potassium carbonate (0.35 mL) was added following the addition of Pd(dppf)Cl_2 (22 mg, 0.036 mmol). The resulting mixture was stirred in a capped glass vial at 149 °C overnight. DMA was removed under reduced pressure, brine was added and the mixture was extracted with ethyl acetate (3 x 30 mL). The organic layers were dried over anhydrous magnesium sulfate, and filtered. The filtrate was concentrated under reduced pressure and the crude product was isolated by silica gel chromatography with Hex/EtOAc gradients to afford a white solid in a 76% yield. ^{1}H NMR (600 MHz, Chloroform-*d*) δ 3.6 (s, 3H), 4.8 (s, 6H), 6.4 (s, 1H), 6.6 (dd, J = 11.0, 2.4 Hz, 1H), 6.7 (td, J = 8.3, 2.4 Hz, 1H), 7.2 (dd, J = 7.4, 5.7 Hz, 2H), 7.3 (d, J = 30.5 Hz, 2H), 7.6 (td, J = 7.7, 1.7 Hz, 2H), 7.7 (dd, J = 8.6, 7.1 Hz, 1H), 8.6 (d, J = 4.4 Hz, 2H).^{13}C-APT NMR (151 MHz, Chloroform-*d*) δ 55.8 (CH_2), 55.8 (CH_3), 95.5 (CH), 95.5 (CH), 99.7 (CH), 107.4 (CH), 107.6 (CH), 122.4 (CH), 124.2 (C), 131.9 (CH), 132.0 (CH), 137.0 (CH), 149.7 (CH), 158.8 (C), 158.8 (C), 162.4 (C), 162.9 (C), 163.4 (C), 163. 7 (C), 165.07 (C). HR-ESI-MS: $[C_{23}H_{22}N_6OF]^+$ 417.1832 HPLC: 100% pure.

6-(2-(methylthio)phenyl)-*N*^{4},*N*^{4}-bis(pyridin-2-ylmethyl)pyrimidine-2,4-diamine(70). 2-(methylthio) benzene boronic acid (0.062 g, 0.369 mmol) was added to a solution of 6-chloro-*N*^{4},*N*^{4}-bis(pyridin-2-ylmethyl)pyrimidine-2,4-diamine (**B-21**) (0.1 g, 0.30 mmol) in THF (2.6 mL), 2 M aqueous sodium carbonate (0.46 mL) was added following the addition of $Pd(PPh_3)_4$ (0.04 g, 0.03 mmol). The resulting mixture was vigorously stirred in reflux overnight. THF was removed under reduced pressure, brine was added, and the mixture was extracted with ethyl acetate (3 x 20 mL). The organic layers were dried over anhydrous magnesium sulfate, and filtered. The filtrate was concentrated on a rotary evaporator. The crude was purified in a silica gel column, using gradients of Hex/EtOAc. Pale powder in a 27% yield. ^{1}H NMR (600 MHz, Chloroform-*d*) δ 8.5 (s, 2H), 7.6 (t, *J* = 7.5 Hz, 2H), 7.3 (dd, *J* = 12.0, 7.6 Hz, 4H), 7.2 (d, *J* = 7.9 Hz, 1H), 7.2 (dt, *J* = 15.0, 6.5 Hz, 3H), 6.2 (s, 1H), 5.0 (d, *J* = 104.2 Hz, 3H), 4.8 (s, 3H), 2.3 (s, 3H).^{13}C- DEPTQ NMR (151 MHz, Chloroform-*d*) δ 16.5 (CH_3), 94.8 (CH), 122.4 (CH), 124.8 (CH), 125.8 (CH), 129.3 (CH), 129.4 (CH), 136.9 (CH), 137.5 (C), 139.0 (C), 162.7 (C), 163.7 (C), 166.0 (C).HR-ESI-TOFMS: $[C_{23}H_{23}N_6S]^+$ 415.1701 HPLC: 96% pure.

6-(2-isopropoxyphenyl)-*N*^{4},*N*^{4}-bis(pyridin-2-ylmethyl)pyrimidine-2,4-diamine (71). 2-isopropoxyphenyl boronic acid (0.15 g, 0.85 mmol) was added to a solution of 6-chloro-*N*^{4},*N*^{4}-bis(pyridin-2-ylmethyl)pyrimidine-2,4-diamine (**B-21**) (0.20 g, 0.60 mmol) in DMA (5.0 mL), 2 M aqueous potassium carbonate (0.91 mL) was added following the addition of Pd(dppf)Cl_2 (45 mg, 0.06 mmol). The resulting mixture was stirred in a capped glass vial at 149 °C for 18 hours. DMA was removed under reduced pressure, brine was added, and the mixture was extracted with ethyl acetate (3 x 20 mL). The organic layers were dried over anhydrous magnesium sulfate, and filtered. The filtrate was concentrated under reduced pressure and the crude product was isolated by silica gel column, ethyl acetate was use to isolate as a pale powder in a 57% of yield. ^{1}H NMR (600 MHz, Chloroform-*d*) δ 8.55 (d, *J* = 4.6 Hz, 2H), 7.86 (dd, *J* = 7.7, 1.7 Hz, 1H), 7.64 (t, *J* = 7.5 Hz, 2H), 7.28 (dd, *J* = 15.5, 1.7 Hz, 3H), 7.17 (dd, *J* = 7.1, 5.2 Hz, 2H), 6.99 (t, *J* = 7.5 Hz, 1H), 6.89 (d, *J* = 8.3 Hz, 1H), 6.70 (s, 1H), 5.03 (s, 3H), 4.86 (s, 2H), 4.47 (hept, *J* = 6.0 Hz, 1H), 1.09 (d, *J* = 6.1 Hz, 6H).^{13}C- DEPTQ NMR (151 MHz, Chloroform-*d*) δ 22.0 (CH_3), 70.7 (CH), 95.5 (CH), 114.5 (CH), 120.9 (CH), 122.3 (CH), 128.9 (C), 130.3 (CH), 130.9 (CH), 136.9 (CH), 145.1 (CH), 155.9 (C), 162.8 (C), 163.2 (C), 163.7 (C). HR-ESI-TOFMS: $[C_{25}H_{27}N_6O]^+$427.2244 HPLC: 99% pure.

6-(2-isobutoxyphenyl)-*N*^{4},*N*^{4}-bis(pyridin-2-ylmethyl)pyrimidine-2,4-diamine (72). 2-isobutoxyphenyl boronic acid (0.27 g, 1.37 mmol) was added to a solution of 6-chloro-*N*^{4},*N*^{4}-bis(pyridin-2-ylmethyl)pyrimidine-2,4-diamine (**B-21**) (0.3 g, 0.9 mmol) in DMA (7.5 mL), 2 M aqueous potassium carbonate (1.365 mL) was added following the addition of Pd(dppf)Cl_2 (67 mg, 0.09 mmol). The resulting mixture was stirred in a capped glass vial at 149 °C for 3 hours. DMA was removed under reduced pressure, brine was added and the mixture was extracted with ethyl acetate (3 x 20 mL). The organic layers were dried over anhydrous magnesium sulfate, and filtered. The filtrate was concentrated under reduced pressure and the crude product was isolated with a silica gel column. The compound came out as a white powder using pure ethyl acetate in a 41% yield. ^{1}H NMR (600 MHz, Chloroform-*d*) δ 8.55 (d, *J* = 4.7 Hz, 2H), 7.78 (dd, *J* = 7.7, 1.6 Hz, 1H), 7.63 (t, *J* = 7.7 Hz, 2H), 7.36 – 7.22 (m, 3H), 7.19 – 7.14 (m, 2H), 7.00 (t, *J* = 7.5 Hz, 1H), 6.91 – 6.86 (m, 1H), 6.64 (s, 1H), 4.96 (s, 3H), 4.81 (s, 2H), 3.68 – 3.64 (m, 2H), 1.80 (hept, *J* = 6.6 Hz, 1H). ^{13}C-DEPTQ NMR (151 MHz, Chloroform-*d*) δ 19.5 (CH_3), 28.3 (CH), 52.9 (CH_2), 75.1 (CH_2), 95.2 (CH), 112.6 (CH), 120.7 (CH), 122.2 (CH), 128.4 (C), 130.3 (CH), 130.7 (CH), 136.9 (CH), 149.7 (CH), 157.1 (C), 162.8 (C), 163.6 (C), 163.7 (C).HR-ESI-TOFMS: $[C_{26}H_{29}N_6O]^+$ 441.2396 HPLC: 99% pure.

6-(2-chlorophenyl)-*N*^{4},*N*^{4}-bis(pyridin-2-ylmethyl)pyrimidine-2,4-diamine (73). 2-chlorophenil boronic acid (0.20 g, 1.28 mmol) was added to a solution of 6-chloro-*N*^{4},*N*^{4}-bis(pyridin-2-ylmethyl)pyrimidine-2,4-diamine (**B-21**) (0.30 g, 0.91 mmol) in THF (7.5 mL), 2 M aqueous sodium carbonate (1.37 mL) was added following the addition of $Pd(PPh_3)_4$ (0.11 g, 0.09 mmol). The resulting mixture was vigorously stirred in reflux overnight. THF was removed under reduced pressure, brine was added, and the mixture was extracted with ethyl acetate (3 x 30 mL). The organic layers were dried over anhydrous magnesium sulfate, and filtered. The filtrate was concentrated on a rotary evaporator. The crude was purified in a silica gel column, using gradients of Hex/EtOAc. Pale powder, 29% yield. ^{1}H NMR (600 MHz, Chloroform-*d*) δ 8.55 (d, *J* = 4.8 Hz, 2H), 7.64 (t, *J* = 6.9 Hz, 2H), 7.47 (dd, *J* = 6.9, 2.4 Hz, 1H), 7.37 – 7.34 (m, 1H), 7.30 – 7.24 (m, 4H), 7.19 – 7.15 (m, 2H), 6.17 (s, 1H), 4.85 (s, 6H).^{13}C-DEPTQ NMR (151 MHz, Chloroform-*d*) δ 95.7 (CH), 122.4 (CH), 127.0 (CH), 128.7 (CH), 129.9 (CH), 130.2 (CH), 130.8 (CH), 132.1 (C), 137.0

(CH), 138.6 (C), 149.7 (CH), 162.8 (C), 163.4 (C), 164.4 (C). HR-ESI-TOFMS: $[C_{22}H_{20}ClN_6]^+$ 403.1429 HPLC 95% pure.

6-(2-fluoro-4-methoxyphenyl)-*N*^{4},*N*^{4}-bis(pyridin-2-ylmethyl)pyrimidine-2,4-diamine (74). 2-fluoro-4-methoxybenzene boronic acid (0.22 g, 1.28 mmol) was added to a solution of 6-chloro-*N*^{4},*N*^{4}-bis(pyridin-2-ylmethyl)pyrimidine-2,4-diamine (**B-21**) (0.3 g, 0.91 mmol) in THF (7.5 mL), 2 M aqueous sodium carbonate (1.36 mL) was added following the addition of $Pd(PPh_3)_4$ (0.106 g, 0.09 mmol). The resulting mixture was vigorously stirred in reflux for 8 hours. THF was removed under reduced pressure, brine was added and the mixture was extracted with ethyl acetate (3 x 30 mL). The organic layers were dried over anhydrous magnesium sulfate, and filtered. The crude was purified in a silica gel column, compound came out Hex/EtAcO 1:4. White solid, 74% yield. ^{1}H NMR (600 MHz, Chloroform-*d*) δ 8.55 (d, *J* = 4.3 Hz, 2H), 7.86 (t, *J* = 8.9 Hz, 1H), 7.63 (t, *J* = 7.5 Hz, 2H), 7.17 (d, *J* = 12.1 Hz, 4H), 6.73 (dd, *J* = 8.8, 2.4 Hz, 1H), 6.58 (dd, *J* = 13.1, 2.4 Hz, 1H), 6.39 (s, 1H), 4.82 (s, 6H), 3.80 (s, 3H).^{13}C-DEPTQ NMR (151 MHz, Chloroform-*d*) δ 55.8 (CH_3), 60.6 (CH_2), 94.3 – 94.4 (d, ^4J = 10.56 Hz, CH), 101.9 – 102.01 (d, ^2J = 26.85 Hz, CH), 110.3 – 110.4 (d, ^4J = 2.89 Hz, CH), 119.1 – 119.2 (d, ^2J = 11.24 Hz, C), 122.4 (CH), 131.3 (d, ^3J = 4.68 Hz, CH), 136.9 (CH), 149.7 (CH), 160.4 (d, ^3J = 2.96 Hz, C), 160.9 – 162.5 (d, ^1J = 251.41 Hz C), 161.8 (d, ^3J = 11.36 Hz, C) 162.9 (C), 163.9 (C). HR-ESI-TOFMS: $[C_{23}H_{22}FN_6O]^+$ 417.1829 HPLC: 98% pure.

***N*^{4}-benzyl-6-(2-methoxyphenyl)-*N*^{4}-(pyridin-2-ylmethyl)pyrimidine-2,4-diamine (75).** 2-Methoxyphenylboronic acid (0.06 g, 0.37 mmol) was added to a solution of *N*^{4}-benzyl-6-chloro-*N*^{4}-(pyridin-2-ylmethyl)pyrimidine-2,4-diamine (**B-5**) (0.10 g, 0.30 mmol) in DMA (2.0 mL), 2 M aqueous potassium carbonate (0.45 mL) was added following the addition of $Pd(dppf)Cl_2$ (22 mg, 0.030 mmol). The resulting mixture was stirred in a capped glass vial at 149 °C for 3.5 hours. DMA was removed under reduced pressure, brine was added and the mixture was extracted with ethyl acetate (3 x 30 mL). The organic layers were dried over anhydrous magnesium sulfate, and filtered. The filtrate was concentrated under reduced pressure and the crude product was filtered through silica gel using ethyl acetate. After purification by column chromatography on silica gel was performed utilizing ethyl acetate to give a white solid in a 83% yield. ^{1}H NMR (600 MHz, DMSO-d_6) δ 8.53 (d, *J* = 4.3 Hz, 1H), 7.77 – 7.73 (m, 1H), 7.71 – 7.68 (m, 1H), 7.33 (q, *J* = 11.5, 9.7 Hz, 5H), 7.27 (dd, *J* = 10.4, 5.8 Hz, 3H), 7.02 – 6.93 (m, 2H), 6.39 (s, 1H), 6.08 (s, 2H), 5.02 (s, 3H), 3.56 (s, 3H). ^{13}C-DEPTQ NMR (151 MHz, DMSO-d_6) δ 55.3 (CH_2), 55.6 (CH_3), 95.74 (CH), 111.6 (CH), 120.2 (CH), 120.2 (CH), 121.0 (CH), 121.5 (CH), 122.0 (CH), 122.3 (CH), 127.4 (CH), 128.4 (C), 128.8 (CH), 130.4 (CH), 130.6 (CH), 137.0 (CH), 145.0 (C), 149.7 (CH), 157.4 (C), 162.9 (C), 163.2 (C), 163.7 (C). HR-ESI-TOFMS: $[C_{24}H_{24}N_5O]^+$ 398.1977 HPLC: 99% pure.

Cell-based functional assays. Generation of stable cell lines previously described[27] to express high levels of the specified receptor and containing the CNiFER were cultured in 10 cm plates with DMEM (Mediatech, Manassas, VA) supplemented with 10% FBS (Gibco) and 1% Glutamine (Gibco), and incubated at 37 °C with 6% CO_2. Cells were selected at 60% confluency and plated the day before using 100 µL of cell suspension per well into black, transparent flat-bottom, TC-treated 96-well plates (Thermo, Waltham, MA; E&K, Greiner Campbell, CA). On the next day, media was replaced with 100 µL of artificial cerebral spinal fluid (aCSF, 121 mM NaCl, 5 mM KCl, 26 mM $NaHCO_3$, 1.2 mM $NaH_2PO_4 \cdot H_2O$, 10 mM glucose, 2.4 mM $CaCl_2$, 1.3 mM $MgSO_4$, 5 mM HEPES, pH 7.4) buffer for cells expressing α4β2 and 5-HT_{3A} receptors. For all assays performed on α7 nAChR CNiFERs, to aCSF buffer PNU-120596 was added at a 10 µM final concentration. Plates were incubated with buffer for 30 min at 37 °C and 6% CO_2. **Quick screen:** The tested compounds were prepared in aCSF for all receptors except α7 nAChR, where 10 µM PNU-120596, a positive allosteric modulator (PAM), was included. The prepared compounds were added in a separate 96-well polypropylene plate (Costar, Corning, NY). Experiments were conducted at 37 °C using 436 nm excitation wavelength. Emitted light was collected at 485 and 528 nm. Basal fluorescence was recorded for 30 s, followed by addition of 50 µL of ligand (first addition). Measurements were made at 3.84 s intervals for 2 min to measure the agonist responses, then followed by application of the control agonist, which was 100 nM (±)-epibatidine (Tocris Bioscience, Bristol, U.K.) for α7 and α4β2 nAChRs, and 3 µM of 5-hydroxytryptamine (5-HT) (Tocris Bioscience, Bristol, U.K.) for the 5HT3A receptor to evaluate the antagonist responses of the test compounds. Agonist and antagonist properties were screened at the final concentration of 13.3 and 10 µM, respectively. Compounds whose fraction of the maximal response (Δ/Δ_{max}) was higher than 0.20 were further evaluated to determine their EC_{50}, whereas compounds that inhibit Δ/Δ_{max} more than 0.50 were further characterized to determine the type of antagonism and calculate the antagonist dissociation constant (K_A).

Agonist assays: Responses were measured in triplicate wells with the FlexStation III (SoftMax Pro 5.2, Molecular Devices) and run at 37 °C by monitoring TN-XXL FRET ratios, emissions of citrine cp174 (527 nm) to eCFP (485 nm), over 120s with agonist injection at 30s. A sigmoidal concentration−response (variable slope) regression of the mean peak FRET ratios was fit to generate concentration−response curves and obtain EC_{50} values (GraphPad Prism 7 for Mac OS X); the plots were normalized to a 316 µM response in α7 nAChR.

Antagonist assays: Tested compounds were prepared in three different concentrations in aCSF, the 96-well plate was divided in four sections (triplicates of each concentration plus the agonist control). The media was replaced by aCSF buffer (first 3 rows) at the 3 concentrations and was incubated for 30 min at 37 °C and 6% CO_2. Agonist was subsequently added and responses were measured in triplicate wells with the FlexStation III (SoftMax Pro 5.2, Molecular Devices) and run at 37 °C by monitoring TN-XXL FRET ratios, emissions of citrine cp174 (527 nm) to eCFP (485 nm), over 120 s with agonist injection at 30s. A sigmoidal concentration−response (variable slope) regression of the mean peak FRET ratios was fit to generate concentration−response curves of control agonist, epibatidine for α7 and α4β2 nAChRs, and 5-HT for 5-HT_{3A}.The K_A for competitive antagonists and noncompetitive antagonists were calculated using the next equations.[52]

$K_A = [A]/[DR - 1]$ (1)

$K_A = [A]/[(\Delta_{max}/\Delta) - 1]$ (2)

where [A] is the concentration of compound, DR (dose ratio) is the EC_{50} ratio of tested compound over the control compound, which is (±)-epibatidine for α7 and α4β2 nAChR, and 5HT for $5HT_{3A}$, and Δ/Δ_{max} is the fraction of the maximal response. Mean values and standard deviations were calculated from at least three independent experiments.

Heterologous Expression of nAChRs in Xenopus Oocytes. The cDNA clones of human nAChR and human resistance-to-cholinesterase 3 (RIC-3) were provided by Dr. Jon Lindstrom (University of Pennsylvania, Philadelphia PA) and Dr. Millet Treinin (Hebrew University, Jerusalem, Israel), respectively. Mouse muscle α1, β1, and δ cDNA clones were provided by Dr. Jim Boulter (Salk Institute, La Jolla CA) and the ε by Dr. Paul Gardner (University of Massachusetts Medical School, Worcester MA). After linearization and purification of the plasmid cDNAs, RNAs were prepared using the mMessage mMachine in vitro RNA synthesis kit (Ambion, Austin, TX). Oocytes were surgically removed from mature female *Xenopus laevis* frogs (Nasco, Ft. Atkinson, WI) and injected with RNAs of nAChR and RIC-3 as described previously.[53] The RIC-3 chaperone protein can improve and accelerate α7 expression with no effects on the pharmacologic properties of the receptors.[52] Frogs were maintained in the Animal Care Service facility of the University of Florida, and all procedures were approved by the University of Florida Institutional Animal Care and Use Committee. All studies were carried out in accordance with the Guide for the Care and Use of Laboratory Animals as adopted and promulgated by the U.S. National Institutes of Health.

Two-Electrode Voltage-Clamp Electrophysiology of Oocytes.

Experiments were conducted using OpusXpress 6000A (Molecular Devices, Union City, CA).[54] Both the voltage and current electrodes were filled with 3 M KCl. Oocytes were voltage-clamped at -60 mV. The oocytes were bath-perfused with Ringer's solution (115 mM NaCl, 2.5 mM KCl, 1.8 mM $CaCl_2$, 10 mM HEPES, and 1 μM atropine, pH 7.2) with a flow rate of 2 ml/min for α7 and 4 ml/min for heteromeric nAChR. To evaluate the effects of experimental compounds on nAChRs expressed in oocytes, two initial control responses to applications of ACh were recorded before test applications of experimental drugs alone or co-applied with the ACh, and test responses were normalized to the average of the two initial control responses for each oocyte. Drug solutions were applied from a 96-well plate via disposable tips. Drug applications were 12 seconds long, followed by a 211-second washout period, for α7 and 6 seconds long, followed by a 271-second washout period, for heteromeric n-AChR. The control concentrations of ACh were 60 μM for wild-type α7, 30μM for α1β1εδ, 100μM for α3β4, 100μM for LS α4β2, and 10μM for HS α4β2. After experimental drug applications, follow-up control applications of ACh were made to determine primed potentiation, desensitization, or rundown of the receptors. Data were collected at 50 Hz, filtered at 20 Hz (α7) or 5 Hz (heteromeric nAChR), and analyzed by Clampfit 9.2 or 10.0 (Molecular Devices) and Excel (Microsoft, Redmond, WA). Data were expressed as means ± S.E.M. from at least five oocytes for each experiment and plotted with Kaleidagraph 4.5.2 (Abelbeck Software, Reading, PA). Concentration-response data were fit to the Hill equation using the Levenberg-Marquardt algorithm. Multicell averages were calculated for comparisons of complex responses. Averages of the normalized data were calculated for each of the 10,322 points in each of the 206.44-second traces (acquired at 50 Hz), as well as the S.E.M. for those averages.

pK_a sample preparation and ^1H NMR parameters.

We utilized a modified version of a previously reported method by Bezeçon *et al.*[44] Samples were analyzed in 0.1 M phosphate buffer (PB) at various pH between 4.0 and 8.5. Compounds were pre-dissolved in DMSO to a 20 mM concentration. Compound **40** was diluted in PB to a 1 mM final concentration and compounds **60** and **74** to a 0.25 mM final concentration in all pH samples. DMSO concentration was 5% or less in every sample. 500 μL of sample was transferred to a 5 mm NMR tube (NORELL) for recording NMR spectra. To avoid having to correct the pH for the presence of deuterium, no deuterated solvent was added to the compound solutions. To provide a lock signal for the NMR spectrometer a sealed 1.7 mm capillary tube filled with DMSO-d_6 was placed in the solution inside the 5 mm NMR tube. The DMSO in the capillary also acted as a chemical shift reference. The water peak in the ^1H NMR spectra was suppressed via pre-saturation or by using a jump-return pulse sequence.[55] Each spectrum was analyzed using Bruker TopSpin 2.1.6. software. The chemical shifts were plotted against pH using GraphPad Prism 7 and the curve was fitted utilizing a sigmoidal concentration−response (variable slope) equation. The inflection point of the sigmoidal curve gave the pK_a of the analyzed ionizable moiety.

ASSOCIATED CONTENT

Supporting Information

The Supporting Information is available free of charge on the ACS Publications website.

Molecular formula strings (.csv)
pKa analysis and chemical characterization (PDF)

AUTHOR INFORMATION

Corresponding Author

* Palmer Taylor, pwtaylor@ucsd.edu

Author Contributions

The manuscript was written through input and contributions of all authors. / All authors have given approval to the final version of the manuscript.

Funding Sources

NIH GM18360, NIH R01 GM57481

Notes

The authors declare no competing financial interest.

ACKNOWLEDGMENTS

We thank Franziska Schnarkowski, Von V Phan, Quynh My Nguyen, Nila Rahmatyan and Joannie Ho, for insightful discussions and contributions. The UCSD Chemistry and Biochemistry Molecular MS facility. Bobby Lucero and Carlo Ballatore for the use of the microwave for synthetic reactions.

ABBREVIATIONS

nAChR, nicotinic acetylcholine receptor; 5-HT, 5-hydroxytryptamine; ACh, acetylcholine; AChBP, acetylcholine

binding protein; aCSF, artificial cerebrospinal fluid; KA, antagonist dissociation constant; DMEM, Dulbecco's modified Eagles media; EtAcO, ethylacetate; DCM, dichloromethane; DMF, dimethylformamide; DMA, dimethylacetamide; DMSO, dimethylsulfoxide; DIPEA, *N,N*-diisopropylethylamine; *m*-CPBA, meta-chloroperbenzoic acid; THF, tetrahydrofuran; LS, low sensitivity form, HS, high sensitivity form; $Pd(dppf)Cl_2$, [1,1′-Bis(diphenylphosphino)ferrocene]dichloropalladium(II); $Pd(PPh_3)_4$, Tetrakis(triphenylphosphine)palladium(0); PAM, positive allosteric modulator; Ago-PAM, agonist-positive allosteric modulator; NMR, nuclear magnetic resonance; mm, millimeter; M, molar; μM, micromolar; nM, nanomolar; PB, phosphate buffer; HEK, human embryonic kidney; CNiFERs, cell-based neurotransmitter fluorescent engineered reporters; 13C-DEPTQ, 13C-distortionless enhancement by polarization transfer quaternary carbons; 13C-APT, 13C-attached proton test; HR-ESI-TOFMS, High resolution Electrospray ionization time-of-flight mass spectrometry.

REFERENCES

(1) Changeux J-P. The nicotinic acetylcholine receptor: a typical 'allosteric machine'. *Philo. Trans. R. Soc. Lond B Biol Sci.* **2018,** 373, 20170174.

(2) Taly, A.; Corringer, P. J.; Guedin, D.; Lestage, P.; Changeux, J. P. Nicotinic receptors: allosteric transitions and therapeutic targets in the nervous system. *Nat Rev Drug Discov.* **2009**, 8, 733-750.

(3) MacDermott, A. B.; Role, L. W.; Siegelbaum, S. A. Presynaptic ionotropic receptors and the control of transmitter release. *Ann Rev Neurosci.* **1999**, 22, 443–485.

(4) Dziewczapolski, G.; Glogowski, C. M.; Masliah, E.; Heinemann, S. F. Deletion of the alpha7 nicotinic acetylcholine receptor gene improves cognitive deficits and synaptic pathology in a mouse model of Alzheimer's disease. *J Neurosci.* **2009**, 29, 8805–8815.

(5) Kem, W. R. The brain α7 nicotinic receptor may be an important therapeutic target for the treatment of Alzheimer's disease: studies with DMXBA (GTS-21). *Behavioural Brain Research*, **2000**, 113, 169-181.

(6) Hoskin, J. L.; Al-Hasan, Y.; Sabbagh, M. N. Nicotinic acetylcholine receptor agonists for the treatment of Alzheimer's dementia: an update. *Nicotine Tob Res.* **2019**, 21, 370-376.

(7) Quik, M.; Kulak, J. M. Nicotine and nicotinic receptors; relevance to Parkinson's disease. *Neurotoxicology*. **2002**, 23, 581-594.

(8) Bordia, T.; Grady, S. R.; McIntosh, J. M.; Quik, M. Nigrostriatal damage preferentially decreases a subpopulation of alpha6beta2* nAChRs in mouse, monkey, and Parkinson's disease striatum. *Mol Pharmacol.* **2007**, 72, 52-61.

(9) Freedman, R.; Olincy, A.; Buchanan, R. W.; Harris, J. G.; Gold, J. M.; Johnson, L.; Allensworth, D.; Guzman-Bonilla, A.; Clement, B.; Ball, M. P.; Kutnick, J.; Pender, V.; Martin, L. F.; Stevens, K. E.; Wagner, B. D.; Zerbe, G. O.; Soti, F.; Kem, W. R. Initial phase 2 trial of a nicotinic agonist in schizophrenia. *Am J Psychiatry*. **2008,** 165, 1040-1047.

(10) Hauser, T.A.; Kucinski, A.; Jordan, K. G.; Gatto, G. J.; Wersinger, S. R.; Hesse, R. A.; Stachowiak, E. K.; Stachowiak, M. K.; Papke, R. L.; Lippiello, P. M.; Bencherif, M. TC-5619: An alpha7 neuronal nicotinic receptor-selective agonist that demonstrates efficacy in animal models of the positive and negative symptoms and cognitive dysfunction of schizophrenia. *Biochem Pharmacol.* **2009**, 78, 803-812.

(11) Bagdas, D.; Gurun, M. S.; Flood, P.; Papke, R. L.; Damaj, M. I. New insights on neuronal nicotinic acetylcholine receptors as targets for pain and inflammation: A Focus on α7 nAChRs. *Curr Neuropharmacol.* **2018**;16, 415-425.

(12) Corradi, J.; Bouzat, C. Understanding the bases of function and modulation of α7 nicotinic receptors: implications for drug discovery. *Mol Pharmacol.* **2016**, 90, 288-299.

(13) Bertrand, D.; Lee, C. H.; Flood, D.; Marger, F.; Donnelly-Roberts, D. Therapeutic potential of α7 nicotinic acetylcholine receptors. *Pharmacol Rev.* **2015**, 67, 1025-1073.

(14) Jones, S.; Sudweeks, S.; Yakel, J. L. Nicotinic receptors in the brain: correlating physiology with function. *Trends Neurosci.* **1999,** 22, 555–561.

(15) Wallace, T. L.; Callahan, P. M.; Tehim, A.; Bertrand, D.; Tombaugh, G.; Wang, S.; Xie, W.; Rowe, W. B.; Ong, V.; Graham, E.; Terry, A. V. Jr.; Rodefer, J. S.; Herbert, B.; Murray, M.; Porter, R.; Santarelli, L.; Lowe, D. A. RG3487, a novel nicotinic α7 receptor partial agonist, improves cognition and sensorimotor gating inrodents. *J Pharmacol Exp Ther.* **2011**, 336, 242-253.

(16) Kalkman, H. O.; Feuerbach, D. Modulatory effects of α7 nAChRs on the immune system and its relevance for CNS disorders. *Cell Mol Life Sci.* **2016**, 73, 2511-2530.

(17) de Jonge, W. J.; Ulloa, L. The alpha7 nicotinic acetylcholine receptor as a pharmacological target for inflammation. *Br J Pharmacol*. **2007**, 151, 915-929.

(18) Horenstein, N. A.; Papke, R. L. Anti-inflammatory silent agonists. *ACS Med Chem Lett*. **2017**, 8, 989-991.

(19) Beers, W. H.; Reich, E. Structure and activity of acetylcholine. *Nature.* **1970**, 228, 917-922.

(20) Horenstein, N. A., Leonik, F. M., and Papke, R. L. Multiple pharmacophores for the selective activation of nicotinic alpha7-type acetylcholine receptors. *Mol. Pharmacol.* **2008**, 74, 1496− 1511.

(21) Umbricht, D.; Keefe, R. S.; Murray, S.; Lowe, D. A.; Porter, R.; Garibaldi, G.; Santarelli, L. A randomized, placebo-controlled study investigating the nicotinic α7 agonist, RG3487, for cognitive deficits in schizophrenia. *Neuropsychopharmacology.* **2014**, 39, 1568-1577.

(22) Prickaerts, J.; van Goethem, N. P.; Chesworth, R.; Shapiro, G.; Boess, F. G.; Methfessel, C.; Reneerkens, O. A. H.; Flood, D. G. Hilt, D.; Gawryl, M.; Bertrand, S.; Bertrand, D.; König, G. EVP-6124, a novel and selective α7 nicotinic acetylcholine receptor partial agonist, improves memory performance by potentiating the acetylcholine responses of α7 nicotinic acetylcholine receptors. *Neuropharmacology.* **2012**, 62, 1099-1110.

(23) Mazurov, A. A.; Kombo, D. C.; Hauser, T. A.; Miao, L.; Dull, G.; Genus, J. F.; Fedorov, N. B.; Benson, L.; Sidach, S.; Xiao, Y.; Hammond, P. S.; James, J. W.; Miller, C. H.; Yohannes, D. Discovery of (2S,3R)-N-[2-(pyridin-3-ylmethyl)-1-azabicyclo[2.2.2]oct-3-yl]benzo[b]furan-2 carboxamide (TC-5619), a selective α7 nicotinic acetylcholine receptor agonist, for the treatment of cognitive disorders. *J Med Chem*. **2012,** 55, 9793-9809.

(24) Kaczanowska, K.; Camacho Hernandez, G. A.; Bendiks, L.; Kohs, L.; Cornejo-Bravo, J. M.; Harel, M.; Finn, M. G.; Taylor, P. Substituted 2-aminopyrimidines selective for α7-nicotinic acetylcholine receptor activation and association with acetylcholine binding proteins. *J. Am. Chem. Soc.* **2017**, 139, 3676-3684.

(25) Brejc, K.; van Dijk, W. J.; Klaassen, R. V.; Schuurmans, M.; van Der Oost, J.; Smit, A. B.; Sixma, T. K. Crystal structure of an ACh-binding protein reveals the ligand-binding domain of nicotinic receptors. *Nature*. **2001**, 41, 269-276.

(26) Kaczanowska, K.; Harel, M.; Radić, Z.; Changeux, J. P.; Finn, M. G.; Taylor, P. Structural basis for cooperative interactions of substituted 2-aminopyrimidines with the acetylcholine binding protein. *Proc Natl Acad Sci U S A*. **2014**, 111, 10749-10754.

(27) Yamauchi, J. G.; Nemecz, A.; Nguyen, T. Q.; Muller, A.; Schroeder, L. F.; Talley, T. T.; Lindstrom, J.; Kleinfeld, D.; Taylor, P. Characterizing ligand-gated ion channel receptors with genetically encoded Ca^{2+} sensors. *PLoS One.* **2011**, 6, 16519.

(28) Zhong, W.; Gallivan, J. P.; Zhang, Y.; Li, L.; Lester, H. A.; Dougherty, D. A. From ab initio quantum mechanics to molecular neurobiology: a cation-pi binding site in the nicotinic receptor. *Proc Natl Acad Sci U S A.* **1998**, 95, 12088-12093.

(29) Quadri, M.; Matera, C.; Silnović, A.; Pismataro, M. C.; Horenstein, N. A.; Stokes, C.; Papke, R. L.; Dallanoce, C. Identification of α7 nicotinic acetylcholine receptor silent agonists based on the spirocyclic quinuclidine-Δ(2)-isoxazoline scaffold: Synthesis and electrophysiological evaluation. *ChemMedChem.* **2017**, 12, 1335-1348.

(30) Papke, R. L.; Horenstein, N. A.; Kulkarni, A.R.; Stokes, C.; Corrie, L. W.; Maeng, C. Y.; Thakur, G. A. The activity of GAT107, an allosteric activator and positive modulator of α7 nicotinic acetylcholine receptors (nAChR), is regulated by aromatic amino acids that span the subunit interface. *J Biol Chem*. **2014,** 289, 4515-4531.
(31) Horenstein, N. A.; Papke, R. L.; Kulkarni, A. R.; Chaturbhuj, G. U.; Stokes, C.; Manther, K.; Thakur, G. A. Critical Molecular Determinants of α7 nicotinic acetylcholine receptor allosteric activation: Separation of direct allosteric activation and positive allosteric modulation. *J Biol Chem*. **2016**, 291, 5049-5067.
(32) Luo, G.; Chen, L.; Poindexter, G. S. Microwave-assisted synthesis of aminopyrimidines. *Tetrahedron Letters.* **2002**, 5739-5742.
(33) Esterhuysen, C.; Heßelmann, A.; Clark, T. Trifluoromethyl: An amphiphilic noncovalent bonding partner. *Chemphyschem.* **2017**, 18, 772-784.
(34) Eccles, K. S.; Elcoate, C. J.; Stokes, S. P.; Maguire, A. R.; Lawrence, S. E. Sulfoxides: potent co-crystal formers. *Crystal Growth & Design,* **2010**, 10, 4243-4245.
(35) Műller, K.; Faeh, C.; Diederich, F. Fluorine in pharmaceuticals: looking beyond intuition. *Science* **2007**, 317, 1881−1886.
(36) Gillis, E. P.; Eastman, K. J.; Hill, M. D.; Donnelly, D. J.; Meanwell, N. A. Applications of fluorine in medicinal chemistry. *J Med Chem*. **2015**, 58, 8315-8359.
(37) Papke RL. Estimation of both the potency and efficacy of alpha7 nAChR agonists from single-concentration responses. *Life Sci.* **2006,** 78, 2812-2819.
(38) Young, G. T.; Zwart, R.; Walker, A. S.; Sher, E.; Millar, N. S. Potentiation of α7 nicotinic acetylcholine receptors via an allosteric transmembrane site. *Proc Natl Acad Sci U S A*. **2008** 105, 14686-14691.
(39) Gulsevin, A.; Papke, R. L.; Stokes, C.; Garai, S.; Thakur, G. A.; Quadri, M.; Horenstein, N. A. Allosteric agonism of α7 nicotinic acetylcholine receptors: Receptor modulation outside the orthosteric Site. *Mol Pharmacol*. **2019**, 95, 606-614.
(40) Gill-Thind, J. K.; Dhankher, P.; D'Oyley, J. M.; Sheppard, T. D.; Millar, N. S. Structurally similar allosteric modulators of α7 nicotinic acetylcholine receptors exhibit five distinct pharmacological effects. *J Biol Chem.* **2015**, 290, 3552-3562.
(41) Papke, R. L; Porter Papke, J. K. Comparative pharmacology of rat and human α7 nAChR conducted with net charge analysis. *Br J Pharmacol.* **2002**, 137, 49-61
(42) Zhou, Y.; Nelson, M. E.; Kuryatov, A.; Choi, C.; Cooper, J.; Lindstrom, J. Human α4β2 acetylcholine receptors formed from linked subunits. *J Neurosci.* **2003**, 23, 9004-9015.
(43) Gift, A. D.; Stewart, S. M.; Bokashanga, P. K. Experimental determination of pKa values by use of NMR chemical shifts, revisited. *Journal of Chemical Education.* **2012,** *89*, 1458-1460.
(44) Bezençon, J.; Wittwer, M. B.; Cutting, B.; Smieško, M.; Wagner, B.; Kansy, M.; Ernst, B. pK_a determination by ^{1}H NMR spectroscopy – An old methodology revisited. *Journal of Pharmaceutical and Biomedical Analysis.* **2014**, 93, 147–155.
(45) Babić, S.; Horvat, A. J. M.; Mutavdžić Pavlović, D.; Kaštelan-Macan, M. Determination of pKa values of active pharmaceutical ingredients. *TrAC Trends in Analytical Chemistry*, **2007,** 26, 1043-1061.
(46) Kerns, E. H. High throughput physicochemical profiling for drug discovery. *J Pharm Sci*. **2001**, 90, 1838-1858.
(47) *in silico* pKa values were calculated using Marvin Sketch Version 17.27.0.
(48) Schiebel, J.; Gaspari, R.; Sandner, A.; Ngo, K.; Gerber, H. D.; Cavalli, A.; Ostermann, A.; Heine, A.; Klebe, G. Charges shift protonation: Neutron diffraction reveals that aniline and 2-aminopyridine become protonated upon binding to trypsin. *Angew Chem. Int Ed Engl.* **2017**, 56, 4887-4890.
(49) Lipinski, C. A.; Lombardo, F.; Dominy, B. W.; Feeney, P. J. Experimental and computational approaches to estimate solubility and permeability in drug discovery and development settings. *Adv. Drug Delivery Rev.* **1997**, 23, 3−25.
(50) Nguyen, V. Q.; Tureček, F. Protonation sites in pyrimidine and pyrimidinamines in the gas phase. J. Am. Chem. Soc. 1997, 119, 2280-2290.
(51) Veber, D. F.; Johnson, S. R.; Cheng, H.-Y.; Smith, B. R.; Ward, K. W.; Kopple, K. D. Molecular Properties That Influence the Oral Bioavailability of Drug Candidates. J. Med. Chem. 2002, 45, 2615− 2623.
(52) Arunrungvichian, K.; Fokin, V. V.; Vajragupta, O.; Taylor, P. Selectivity optimization of substituted 1,2,3-triazoles as α7 nicotinic acetylcholine receptor agonists. ACS Chem Neurosci. 2015, 6, 1317-1330.
(53) Halevi, S.; Yassin, L.; Eshel, M.; Sala, F.; Sala, S.; Criado, M.; Treinin, M. Conservation within the RIC-3 gene family. Effectors of mammalian nicotinic acetylcholine receptor expression. J Biol Chem. 2003, 278, 34411–34417.
(54) Papke, R. L.; Stokes, C. Working with opusxpress: methods for high volume oocyte experiments. Methods. 2010, 51, 121-133.
(55) Plateau, P. Gueron, M. Exchangeable proton NMR without base-line distortion, using new strong-pulse sequences. J. Am. Chem. Soc. 1982, 104, 7310-7311.
(56) All structures were drawn using ChemDraw professional version 17.1.1.0.

Insert Table of Contents artwork here

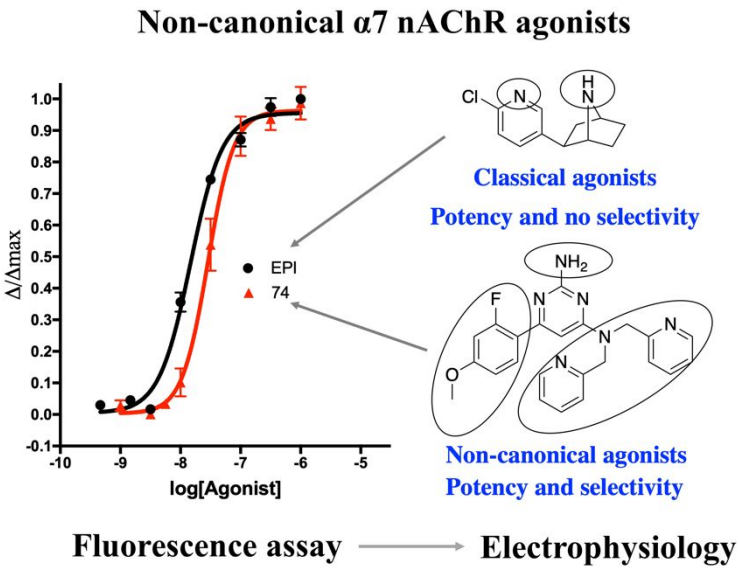
Non-canonical α7 nAChR agonists
Δ/Δmax
log[Agonist]
EPI
74
Classical agonists
Potency and no selectivity
Non-canonical agonists
Potency and selectivity
Fluorescence assay
Electrophysiology